SHORT TITLE

Knockout of trichome-regulating MYBs in poplar

ARTICLE TITLE

Multiplex knockout of trichome-regulating MYBs in poplar affects light sensitivity and triterpene accumulation

ONE SENTENCE SUMMARY

Non-glandular trichomes in poplar have roles both as a physical barrier and a chemical factory to mediate plant interactions with the environment.

AUTHORS

W. Patrick Bewg[1,2,3], Scott A. Harding[1,2,3], Nancy L. Engle[4], Brajesh N. Vaidya[5,a], Jingyin Yu[1,b], Ran Zhou[1,2,3], Jacob Reeves[6,c], Thomas W. Horn[6], Nirmal Joshee[5], Jerry W. Jenkins[7,8], Shengqiang Shu[8], Kerrie W. Barry[8], Yuko Yoshinaga[8], Jane Grimwood[7,8], Robert J. Schmitz[2], Jeremy Schmutz[7,8], Timothy J. Tschaplinski[4], and Chung-Jui Tsai[1,2,3*]

[1] *School of Forestry and Natural Resources, University of Georgia, Athens, Georgia, 30602, USA*

[2] *Department of Genetics, University of Georgia, Athens, Georgia, 30602, USA*

[3] *Department of Plant Biology, University of Georgia, Athens, Georgia, 30602, USA*

[4] *Oak Ridge National Laboratory, Oak Ridge, Tennessee, 37830, USA*

[5] *Fort Valley State University, Fort Valley, Georgia, 31030, USA*

[6] *Department of Computer Science, University of Georgia, Athens, Georgia, 30602, USA*

[7] *HudsonAlpha Institute for Biotechnology, Huntsville, Alabama, 35806, USA*

[8] *U.S. Department of Energy Joint Genome Institute, Berkeley, California, 94720, USA*

**Senior author and author for correspondence: cjtsai@uga.edu (C.-J.T.)*

[a] *Present address: GreenVenus, LLC, Wimauma, Florida 33598, USA*

[b] *Present address: Boyce Thompson Institute, Cornell University, Ithaca, New York 14853, USA*

[c] *Present address: SoundHound Inc., Boulder, Colorado 80302, USA*

The author responsible for distribution of materials integral to the findings presented in this article in accordance with the policy described in the Instructions for Authors is Chung-Jui Tsai (cjtsai@uga.edu).

AUTHOR CONTRIBUTIONS

C.-J.T. and W.P.B. conceived the study and designed the experiments; W.P.B. performed all experiments and analyzed data; S.A.H. provided guidance on physiological and metabolic analyses; J.Y., J.R., T.W.H, and R.Z. provided bioinformatic support; B.N.V. and N.J. performed SEM analysis; J.J., K.B., R.J.S., Y.Y., S.S., J.G. and J.S. contributed the *Populus tremula* x *P. alba* INRA 717-1B4 draft genome; N.L.E. and T.J.T. performed wax compositional analysis; W.P.B. wrote the manuscript, C.-J.T. revised the manuscript with input from S.A.H.

FUNDING

The work was funded in part by The Center for Bioenergy Innovation, a U.S. Department of Energy Research Center supported by the Office of Biological and Environmental Research in the DOE Office of Science, the Division of Integrative Organismal Systems (grant nos. IOS-1546867) of the National Science Foundation, the Community Science Program of the Joint Genome Institute, a DOE Office of Science User Facility. The work conducted by the U.S. Department of Energy Joint Genome Institute is supported by the Office of Science of the U.S. Department of Energy under Contract No DE-AC02-05CH11231.

Keywords: multiplex editing, gene duplication, triterpenes, sterol, glabrous, genomic dropout

ABSTRACT

Hair-like trichomes cover the aerial organs of many plant species and act as a barrier between a plant and its environment. They function in defense against biotic and abiotic stresses, while also serving as sites for synthesis and storage of secondary metabolites. Previously, the transcription factor PtaMYB186 was identified as a positive regulator of trichome initiation during early stages of leaf development in *Populus tremula* x *P. alba* (IRNA 717-1B4). However, trichome regulation in poplar remains largely unexplored, as does the functional redundancy of duplicated poplar genes. Here, we employed CRISPR/Cas9 to target a consensus region of *PtaMYB186* and its close paralogs for knockout. Regeneration of glabrous mutants suggested their essential roles in poplar trichome development. No apparent differences in growth and leaf transpiration rates between the mutants and the controls were observed, but trichomeless poplars showed increased insect pest susceptibility. RNA-seq analysis revealed widespread down-regulation of circadian- and light-responsive genes in the mutants. When exposed to a high light regime, trichomeless mutants accumulated significantly higher levels of photoprotective anthocyanins. Cuticular wax and whole leaf analyses showed a complete absence of triterpenes in the mutants, suggesting biosynthesis and storage of triterpenes in poplar occurs in the non-glandular trichomes. This work also demonstrates that a single gRNA with SNP-aware design is sufficient for multiplex targeting of paralogous genes in outcrossing and/or hybrid species with unexpected copy number variations.

INTRODUCTION

Trichomes are modified epidermal cells giving a hair-like appearance to the aerial surfaces of shoot organs throughout the Plantae kingdom. The abundance and morphological diversity of trichomes reflect their multifunctionality, including protection against feeding insects, excessive transpiration, and UV radiation (Schuepp, 1993; Bickford, 2016). Trichomes can be subclassified as unicellular or multicellular, branched or unbranched, and glandular or non-glandular (Payne, 1978). Glandular trichomes are known for their ability to synthesize, store and secrete large quantities of specialized metabolites, especially terpenoids, some with insecticidal or pharmaceutical properties (Schuurink and Tissier, 2020). Non-glandular trichomes, on the other hand, are present in a wide range of plant taxa, including *Arabidopsis* and *Populus* spp., and are known to synthesize and store predominantly phenolics but do not possess secretory abilities (Karabourniotis et al., 2020).

Trichome initiation and development are under strict spatiotemporal regulation (Larkin et al., 2003; Hülskamp, 2004). Despite trichome diversity, the main molecular and hormonal pathways governing their development appear conserved in angiosperms (Fambrini and Pugliesi, 2019). For instance, exogenous jasmonic acid (JA), cytokinin and gibberellin (GA) applications promote trichome initiation of both unicellular (*e.g.*, *A. thaliana*) and multicellular (*e.g.*, *Medicago truncatula* and *P. trichocarpa*) types (Maes and Goossens, 2010). The phytohormonal actions are mediated in part through the “MBW” transcription activation complex, consisting of interacting R2R3-MYB and bHLH (basic helix-loop-helix) transcription factors on a WD40 repeat protein scaffold (Maes et al., 2008; Zhao et al., 2008). The MBW complex modulates not only trichome development but also several other traits, including root hair patterning and anthocyanin biosynthesis (Wang and Chen, 2014; Fambrini and Pugliesi, 2019). In Arabidopsis, the single-copy WD40 protein TTG1 (TRANSPARENT TESTA GLABRA1) is involved in all MBW-mediated processes (Walker et al., 1999), whereas three bHLHs participate in a partially redundant manner (Zhang et al., 2003). MYB, on the other hand, is the most discriminating component of the complex, with structurally distinct R2R3-MYB and R3-MYB members competing for bHLH binding to promote or inhibit trichome development, respectively (Wang and Chen, 2014). Even among R2R3-MYBs, functional specialization is evident such that constitutive expression of anthocyanin-associated *MYBs* cannot phenotypically rescue the Arabidopsis *glabrous1* (*gl1*) mutant and vice versa (Zhang and Hülskamp, 2019).

Previously, activation-tagging has identified PtaMYB186 as a positive regulator of trichome development in *Populus tremula* x *P. alba* INRA 717-1B4, hereon referred to as 717 (Plett et al., 2010). PtaMYB186 is orthologous to Arabidopsis AtMYB106 whose loss-of-function mutations result in mutants (*noeck* or *nok*) with glassy and highly branched trichomes (Folkers et al., 1997). Initially proposed to function in negative regulation of epidermal outgrowth and trichome branching (Jakoby et al., 2008; Gilding and Marks, 2010), AtMYB106 and its paralogous AtMYB16 were later found to also regulate cuticle development and wax crystal accumulation in Arabidopsis (Oshima et al., 2013). The *Antirrhinum majus* ortholog AmMIXTA controls epidermal conical cell formation in petals and promotes multicellular trichome development when overexpressed in tobacco (*Nicotiana tabacum*) (Glover et al., 1998). A similar role was reported for the cotton (*Gossypium hirsutum* L.) ortholog GhMYB25 which regulates specialized epidermal cell outgrowth of trichome and cotton fibers (Machado et al., 2009). These results underscore both pleiotropic and specialized functions of MYBs in diverse epidermal cell developmental programs both within and across species.

In the case of poplar, *PtaMYB186* corresponds to gene model Potri.008G089200 in the *P. trichocarpa* v3 genome. It belongs to clade 15 of the R2R3-MYB protein family tree (Wilkins et al., 2009), which also includes AtMYB106 and AtMYB26, but is distinct from the other trichome-related MYBs (AtGL1 and AtMYB23) in clade 45. Clade 15 is expanded in poplar and contains three additional members, MYB138, MYB38 and MYB83, with as yet unclear functions (Plett et al., 2010). The current research employed CRISPR/Cas9 to knock out (KO) *PtaMYB186* and its close paralogs, *PtaMYB138* and *PtaMYB38* in poplar 717. Analysis of the resulting glabrous mutants substantiates their essential involvement in poplar trichome development. Plant growth, physiology, transcriptome and metabolite data were synthesized to infer trichome functions in poplar. We also discuss technical findings associated with CRISPR editing of duplicated genes.

RESULTS

Multiplex CRISPR/Cas9 editing of trichome-regulating MYBs

The four *P. trichocarpa* MYB genes in clade 15 are derived from multiple duplication events, including an ancient (gamma) whole genome duplication (*MYB186* and *MYB83*), a Salicoid duplication (*MYB186* and *MYB38*), and a tandem duplication (*MYB186* and *MYB138*) (Figure 1). MYB186, MYB138 and MYB38 share higher levels (88-96%) of amino acid sequence similarity than with MYB83 (55-57%). To ascertain these MYB involvement in trichome development, we mined RNA-seq data from different stages of 717 leaf development. Transcript levels of *MYB186*, *MYB138* and *MYB38* were highest in newly emerged leaves (Leaf Plastochron Index LPI-1) when trichome initiation occurs (Plett et al., 2010), but quickly declined thereafter in expanding (LPI-5) and mature (LPI-15) leaves (Figure 1). In contrast, *MYB83* transcripts were detected throughout leaf maturation (Figure 1), weakening support for its potential involvement in trichome development.

We designed a single gRNA to target a conserved region in exon two of *MYB186*, *MYB138* and *MYB38* (Figure 2A) based on the *P. trichocarpa* v3.0 reference genome and cross-checked using the 717 variant database (Xue et al., 2015; Zhou et al., 2015) to assure the gRNA target sites were SNP-free in 717. Two CRISPR/Cas9 constructs were generated (see Methods); the first erroneously omitted a guanine between the gRNA and the scaffold sequences (referred to as ΔG, Figure 2B), which was corrected in the second construct (Figure 2A). Both constructs were used for 717 transformation in order to learn whether ΔG would affect CRISPR/Cas9 editing. In total, 28 independent events generated from the ΔG construct were all phenotypically indistinguishable from the wild type (WT) and Cas9-only controls (Figure 2C-J). In contrast, 37 independent events generated from the correct KO construct were glabrous (Figure 2N-R), and one single event (KO-27) had a greatly reduced number of trichomes (Figure 2K-M). SEM imaging revealed no trichome initiation or development on the abaxial leaf surface of the glabrous mutants (Figure 2Q). Epidermal cell morphology of young leaves from tissue cultured plants did not differ between control and mutant genotypes on either their abaxial (Figure 2F, N) or adaxial surfaces (Figure 2J, R). These results are consistent with roles for MYB186 (Plett et al., 2010) and its paralogs MYB138 and MYB38 in trichome initiation and development.

Mutation spectrum of duplicated 717 *MYB* alleles

A random selection of 30 glabrous KO events, 28 ΔG events, two Cas9-only events and four WT plants were subject to amplicon deep-sequencing using consensus primers for *MYB186*, *MYB138* and *MYB38*. Initial analysis by AGEseq (Xue and Tsai, 2015) showed numerous chimeric edits (mix of edited and unedited sequences at a given site) not observed in other CRISPR/Cas9-edited 717 transgenics in our experience (Zhou et al., 2015; Bewg et al., 2018). *De novo* assembly of amplicon reads from control samples revealed seven distinct sequences, more than the expected six alleles of the three target genes. Blast search against the preliminary 717 genome assemblies by the Joint Genome Institute uncovered an unexpected copy number variation in 717 relative to the *P. trichocarpa* reference genome. The region containing paralogous *MYB186* and *MYB138* on Chromosome (Chr) 8 is found as a tandem duplicate in one of the 717 subgenomes (Figure 3A). This results in three alleles each for *MYB186* and *MYB138* (two on the main subgenome [Chr8m] and one on the alternative subgenome [Chr8a]) and two alleles for *MYB38* on Chr10 (Chr10m and Chr10a, Figure 3A). Two of the eight alleles were identical in the amplicon region, explaining the seven distinct sequences we recovered from *de novo* assembly. Based on the 717 assemblies, we redesigned primers to ensure the amplicons span allele-specific SNP(s) to aid mutation pattern determination of the eight alleles.

Amplicon-sequencing showed no editing in the 28 ΔG events, except one (ΔG-24) with a 9 bp deletion at one of the eight target sites (Dataset S1). This translates into a mutation rate of 0.45% (one out of 224 potential target sites), which suggests a negative effect of the ΔG on CRISPR/Cas9 function (hereafter, the ΔG plants were treated as transformation controls). In contrast, we confirmed successful editing across the eight alleles in all glabrous mutants except KO-27 (Figure 3B, Dataset S1). This event showed six edited and two intact (unedited) alleles, consistent with trichome detection in this line (Figure 2K-M). In aggregate, small insertions and deletions (indels) were the predominant edits at all sites (Figure 3B-C), with frameshift deletions of 1 bp (-1), 2 bp (-2) and 4 bp (-4) accounting for over three quarters of the indel mutations (Figure 3C). In-frame deletions (-3 or -6) accounted for 10% of indels and were detected in 14 events, including KO-27 (Figure 3B-C). These in-frame mutations are unlikely functional because the gRNA target site is located within the third α-helix of the R2 domain critical for MYB-DNA interaction (Wang et al., 2020), and because 13 of the events with in-frame mutations are glabrous. We therefore conclude that all small indels we detected are null mutations.

The vast majority (80%) of the mutants also harbored potentially large deletions as evidenced by the dearth of mapped amplicon reads at the target sites, referred to as no-amplification (NA) alleles (Figure

3B-C). The NA frequencies differed by chromosome position and were positively correlated with copy number, being highest at the Chr8m site (four tandem copies), followed by the Chr8a site (two tandem copies) and least at the single-copy Chr10 sites (Figure 3A-B). The NA alleles on Chr8 often spanned consecutive copies, suggesting large dropouts between two gRNA cleavage sites. To support this idea, we examined a subset of mutant lines using allele-specific primers for PCR amplification of the target genes (Figure S1). As expected, NA alleles yielded no PCR products, whereas alleles previously detected by amplicon sequencing produced observable PCR products (Figure S1). We next used consensus primers for PCR amplification of all six Chr8 (*MYB186* and *MYB138*) alleles, approximately 850 – 950 bp, from three control plants and four KO lines each with 4-5 NA alleles on Chr8. These KO lines had reduced PCR band intensity when compared with controls (Figure 3D). Sanger sequencing of the PCR products resulted in clean chromatograms with clear nucleotide peaks throughout the sequenced length for KO-5 and KO-69 (Figure 3E), two mutant lines with only one detectable Chr8 allele (Figure 3B). In contrast, the chromatograms for KO-63, KO-70 (both containing two detectable Chr8 alleles) and WT samples were noisy as would be expected for mixed template (Figure 3E). The Sanger sequencing data of KO-5 and KO-69 not only confirmed the indel pattern (-2 in both cases) detected by amplicon sequencing, but also supported the occurrence of gene fusion between two gRNA cleavage sites, based on SNP patterns upstream and downstream of the gRNA target (Figure 3B, E). KO-5 harbors a fusion junction between *MYB186m1* and *MYB138m1* with a ~29 Kb genomic dropout, whereas KO-69 contains a fusion of *MYB138m1* and *MYB138m2* with a ~62 Kb genomic dropout (Figure 3E, Figure S2). Together, our findings show that a single gRNA is highly effective for multiplex KO of tandem duplicates via either small indels or large deletions.

Growth, leaf transpiration and insect response of glabrous mutants

The trichome mutation did not impact growth rate as plant height and stem diameter were comparable to the controls over a seven-week period under glasshouse conditions (Figure 4A-B). Stem and leaf dry biomass also did not differ significantly between controls and mutants (Figure 4C-D). As trichomes can influence transpiration by acting as a barrier between the leaf and its environment (reviewed in Karabourniotis et al., 2020), we monitored transpiration-driven water uptake via petiole feeding and also leaf water loss during benchtop drying. Transpiration rates were measured using mature leaves (LPI-10 to LPI-15) of growth chamber plants either matched by size (whole leaf), or trimmed with a stencil 24 hours in advance to control for leaf area. No differences were seen in water uptake over six hours for whole leaves (p=0.48) or trimmed leaves (p=0.38) (Figure 4E). We also detected no differences

in rate of water loss between glasshouse-grown mutants and controls for LPI-6 (p=0.68) or LPI-20 (p=0.16) over a three-hour drying period, though higher variation was observed in younger leaves overall (Figure 4F). The trichomeless mutants were more susceptible to thrip damage than controls, consistent with a role of trichomes in defense against insect pests (Figure S3).

Altered expression of genes involved in development and hormonal responses in trichomeless leaves

We next investigated transcriptomic changes in trichomeless leaves, focusing on expanded leaves (LPI-6) post trichome initiation. We confirmed, as anticipated based on their developmental profiles (Fig. 1), that *MYB186*, *MYB138* and *MYB38* were no longer expressed in LPI-6 of WT and ΔG controls (Table S1). The ancient duplicate *MYB83* was well expressed in LPI-6 and unaffected in the glabrous mutants (Table S1), excluding its involvement in trichome development.

Differential expression (DE) analysis identified 319 significantly up-regulated and 469 down-regulated genes ($p \leq 0.01$, fold change ≥ 1.5, RPKM ≥ 3) in trichomeless LPI-6 when compared with controls (Dataset S2). Among those up-regulated were genes encoding orthologs of other trichome regulators, such as kinesin-interacting calcium-binding protein (KIC) and zinc finger protein GLABROUS INFLORESCENCE STEMS (GIS) (Figure 5A). GIS acts upstream of the MBW complex (Gan et al., 2006), whereas KIC regulates post-initiation microtubule-associated trichome morphogenesis (Oppenheimer et al., 1997; Reddy et al., 2004). In addition, genes encoding putative negative regulators of trichome branching were significantly down-regulated in the trichomeless mutants (Figure 5A), including ubiquitin-protein ligase3 (UPL3; Downes et al., 2003), calpain-type cysteine protease (DEFECTIVE KERNEL1 or DK1; Galletti et al., 2015) and guanine nucleotide exchange factor (SPIKE1; Qiu et al., 2002). Misregulation of these genes may reflect multiple compensatory responses to compromised trichome development in the mutants.

DE genes that were up-regulated in the glabrous leaves showed a significant enrichment of Gene Ontology (GO) terms associated with various hormonal responses (Figure 5B). Specifically, genes involved in GA biosynthesis and perception (Mauriat and Moritz, 2009), as well as JA biosynthesis, turnover and signaling (Widemann et al., 2013) were significantly up-regulated (Figure 5A). These findings are consistent with synergistic involvement of GA and JA in promoting trichome formation (Qi et al., 2011), and with compensatory responses of glabrous mutants to trichome inhibition. In contrast, we observed an overrepresentation of “shoot system morphogenesis” among DE genes down-regulated

in the mutants (Figure 5B). For example, genes encoding orthologs of *Arabidopsis* TOPLESS-RELATED3 (TPR3), a corepressor implicated in several developmental programs (Long et al., 2006; Tao et al., 2013), and its potential interacting partner (SUPPRESSOR OF MORE AXILLARY GROWTH2-LIKE or SMXL) (Soundappan et al., 2015) were significantly down-regulated in the mutants (Figure 5A). Also down-regulated were orthologs of known developmental regulators involved in seedling morphogenesis (*RADIALIS-LIKE SANT/MYB3*, *RSM3*) (Hamaguchi et al., 2008) and leaf development, such as *ROTUNDIFOLIA-LIKE14* (*RTFL14*) (Narita et al., 2004; Wen et al., 2004) and *TCP2-1* (*TEOSINTE BRANCHED1/CYCLOIDEA/PROLIFERATING CELL FACTOR*) (Cheng et al., 2021) (Figure 5A). These data add to a growing body of evidence that trichome development shares transcriptional and hormonal regulation with other developmental processes (Matías-Hernández et al., 2016).

Circadian and light-regulated gene expression in trichomeless mutants

We observed an overrepresentation of GO terms associated with chloroplast organization, photosynthesis, circadian rhythm, phototropism, and various light responses within the down-regulated DE genes, and responses to osmotic stress and wounding, water transport and metal ion transport within the up-regulated DE genes (Figure 5B). Many of the overrepresented GO terms are consistent with the roles of trichomes as a barrier to wounding, transpiration and light absorbance. We detected significantly decreased transcript levels of orthologs involved in circadian clock regulation, including *GIGANTEA* (*GI*, Park et al., 1999), *JUMONJI DOMAIN* (*JMJD5*, Jones et al., 2010), *TIME FOR COFFEE* (*TIC*, Hall et al., 2003) and *PSUEDO-RESPONSE REGULATOR5* (*PRR5*, Matsushika et al., 2000) (Figure 5C). Diurnal expression of these genes has been previously reported in poplar leaves (Filichkin et al., 2011). Many of these proteins are known to integrate light signaling and circadian rhythm to affect photomorphogenesis (Ni, 2005). Indeed, genes encoding blue light receptors phototropins (PHOT1 and PHOT2, Briggs et al., 2001) were down-regulated in the mutants (Figure 5C), as were components of blue light-dependent circadian cycles, namely GI and flavin-binding kelch repeat F box protein (FKF, Imaizumi et al., 2003) (Figure 5C). Widespread downregulation was also observed for orthologs involved in photosystem I (PSI) and PSII, chlorophyll biosynthesis and chloroplast import apparatus (Dataset S2), suggesting numerous chloroplast processes were impacted in the absence of trichomes.

Consistent with altered light responses, we frequently observed red coloration of young glabrous leaves when plants neared supplemental lights. To further explore this, plants were grown under high-light conditions, and as expected, mutant leaves developed an intense red color (Figure 6) indicative of

anthocyanins, a photoprotective flavonoid (Smillie and Hetherington, 1999). The glabrous mutants produced significantly higher levels of anthocyanins in LPI-3 and marginally so in LPI-5, but not in LPI-15 farther down and likely shielded by upper leaves (Figure 6C). The results suggest elevated anthocyanin biosynthesis as a photoprotective mechanism in the glabrous mutants.

Absence of triterpenes in trichomeless leaves

Trichomes as epidermal outgrowths are covered with waxy cuticles like other epidermis cells (Hegebarth et al., 2016). We thus investigated whether leaf surface wax load and composition differed between control and trichomeless plants. Total wax load of mature leaves did not change significantly between genotypes (Figure 7A). Alkanes were the most abundant class of leaf cuticular waxes detected in 717 and differed little between control and trichomeless plants (Figure 7B). In contrast, levels of triterpenes, fatty alcohols and β-sitosterol were significantly reduced in the mutants (Figure 7B-D). Specifically, the wax of mutant leaves was devoid of any triterpenes, including α-amyrin, β-amyrin, β-amyrone and lupenone (Figure 7E). Two primary alcohols, 1-octacosanol (C28) and 1-hexacosanol (C26), were depleted in the mutants by >50% (Figure 7C), and β-sitosterol, by 42% (Figure 7D). To further investigate the absence of triterpenes in the mutant wax, whole leaf tissues were also profiled for compounds that were significantly reduced in cuticular wax. Again, triterpenes were not detected in the leaves of trichomeless mutants (Figure 7E), whereas 1-octacosanol, 1-hexacosanol and β-sitosterol were detected at levels comparable with controls (Figure 7C, D). The lack of triterpenes in the trichomeless leaves thus suggests triterpene biosynthesis occurs within the non-glandular trichomes of 717.

We then examined the whole-leaf RNA-seq data for molecular evidence in support of altered wax composition in the mutants (Figure 7F). Orthologs of known triterpene biosynthetic genes (Thimmappa et al., 2014) were found to be poorly expressed in the leaves we sampled for both controls and mutants. This may reflect a dilution effect of trichome-specific transcripts in the whole-leaf transcriptome or suggest triterpene biosynthesis has already ceased in LPI-6. The trichomeless leaves exhibited significant down-regulation of *PtaSTE1.1* (Potri.004G097500), encoding a Δ^7-sterol-C_5-desaturase orthologous to *Arabidopsis* AtSTE1 involved in sterol biosynthesis (Gachotte et al., 1995), and of *PtaFAR3.1* (Potri.004G185000), encoding a fatty acyl-CoA reductase orthologous to *Arabidopsis* AtFAR3 (also called ECERIFERUM4 or CER4) involved in the synthesis of primary alcohols for cuticular wax formation (Rowland et al., 2006). However, transcript levels of their respective genome duplicates, *PtaSTE1.2* (Potri.017G116600) and *PtaFAR3.2* (Potri.009G145000), remained unchanged (Figure 7F). Such

352 discrepancies were also observed among genome duplicates of several other fatty acid biosynthetic
353 genes (Figure 7F). In *Arabidopsis* rosette leaves, wax biosynthesis and composition have been shown to
354 differ between trichomes and pavement cells (Hegebarth et al., 2016); for example, *AtFAR3* expression
355 is restricted to trichomes (Rowland et al., 2006). The specific down-regulation of *PtaSTE1.1* and
356 *PtaFAR3.1* in glabrous leaves may therefore hint at their preferential involvement in trichome wax
357 biosynthesis.
358
359
360 **DISCUSSION**
361 The role of trichomes in pest deterrence, transpiration and light absorbance and reflectance is well
362 documented (Bickford, 2016; Karabourniotis et al., 2020). Previously, elevated expression of *PtaMYB186*
363 in 717 was shown to increase trichome density, resulting in increased growth, leaf transpiration,
364 stomata conductance, gas exchange and resistance to feeding insects (Plett et al., 2010). In the present
365 study, CRISPR/Cas9-KO of *PtaMYB186* and its paralogs *PtaMYB138* and *PtaMYB38* resulted in the
366 complete absence of trichomes on stem, leaf and petiole surfaces. An increased pest susceptibility in the
367 glabrous poplar was observed. However, no significant differences in growth or transpiration were
368 detected under the experimental conditions. Further research under field conditions may be required to
369 fully explore the relationship between water use, growth and trichome coverage in poplar.
370
371 Transcriptome profiling results support an intricate role of trichomes in photoresponses, as glabrous
372 leaves showed widespread down-regulation of genes involved in circadian rhythms, photoreception, and
373 photomorphogenesis. The trichomeless mutants also exhibited increased sensitivity to light, and
374 hyperaccumulated anthocyanins in the upper leaves under high light regimes. The results are in
375 agreement with trichomes and anthocyanins both acting as light screens (Liakopoulos et al., 2006), and
376 point to increased anthocyanin accrual as a compensatory photoprotective response in the glabrous
377 mutants. As anthocyanin biosynthesis is also regulated by the MBW complex (Ramsay and Glover, 2005),
378 accumulation of anthocyanins in the KO mutants rules out the involvement of MYB186, MYB138 and
379 MYB38 in poplar anthocyanin biosynthesis.
380
381 The glabrous mutants provide strong support for an essential role of PtaMYB186/138/38 in trichome
382 development of 717. Loss of trichomes did not significantly affect the total epidermal wax load, but led
383 to a complete absence of triterpenes both in cuticular wax and whole leaves of the mutants. The results

384 do not support a role for these MYBs in cuticle development in poplar as has been reported for their
385 Arabidopsis orthologs AtMYB106 and AtMYB16 (Oshima et al., 2013), and hint at functional divergence
386 of clade 15 MYBs between these two species. Although we cannot rule out a direct involvement of
387 MYB186/138/38 in triterpene biosynthesis (*i.e.*, lack of triterpenes as a direct KO effect), MYBs that have
388 been implicated in triterpene regulation belong to phylogenetically distinct clades (Wilkins et al., 2009;
389 Falginella et al., 2021). The absence of triterpenes in trichomeless leaves led us to suggest trichomes as
390 sites of triterpene biosynthesis and storage in poplar. While glandular trichomes are well known for
391 their roles in biosynthesis and storage of terpenes (Lange and Turner, 2013; Lange and Srividya, 2019),
392 there is only limited reporting of terpenes in non-glandular trichomes in *Artemisia annua* (Wang et al.,
393 2009; Soetaert et al., 2013) and Lamiaceae and Verbenaceae species (dos Santos Tozin et al., 2016).
394 Detection of triterpenes in poplar with non-glandular trichomes thus adds to the growing body of
395 evidence for this conserved function.
396
397 This study demonstrates that a single gRNA targeting conserved genomic sites is highly effective for
398 multiplex editing, despite the unexpected genomic complexity in hybrid 717. The population of 30
399 independent KO lines experienced an average of 5.4 cleavages per line based on indel alleles, which is
400 likely an underestimate because many NA alleles also resulted from cleavages as shown for KO-5 and
401 KO-69 (Figure 3). The work highlights the importance of ensuring SNP-free targets for gRNA design when
402 working within a highly heterozygous genome (Zhou et al., 2015). Additionally, the negligible editing by
403 the ΔG construct provides insight into scaffold structure and stability. The ΔG configuration can lead to
404 two hypothetical outcomes: either the guanine is omitted from the scaffold and the gRNA remains intact
405 and capable of base pairing to the target sites for Cas9 cleavage, or the guanine is sequestered for
406 secondary structure folding of the scaffold, resulting in a 3'-truncated gRNA no longer PAM-adjacent at
407 the target sites (Figure 2B). The lack of mutations in ΔG transformants supports the latter scenario and is
408 consistent with transcription and folding of gRNA molecules preceding their base-pairing with genomic
409 targets. Moreover, the low trichome density of KO-27 suggests that MYB38 plays a redundant but minor
410 role in leaf/stem trichome initiation. Follow-up research, including use of CRISPR to address the allele
411 dose-response, is needed to dissect the functional redundancy of clade 15 MYB members more fully.
412 Finally, the unedited (WT) *MYB38* alleles in KO-27 appear stable during vegetative propagation as this
413 event has maintained a low trichome density for over two years in both tissue culture and greenhouse
414 environments. This contributes to previously reported stability of CRISPR editing outcomes in clonally
415 propagated poplar (Bewg et al., 2018).

MATERIALS AND METHODS

Generation of KO mutants

The ΔG and KO constructs in p201N-Cas9 (Jacobs et al., 2015) were prepared by Gibson assembly. PCR was used to amplify the p201N-Cas9 binary vector following *Swa*I (New England BioLabs) digestion, and the *Medicago truncatula Mt*U6.6 promoter and scaffold fragments from HindIII and EcoRI (New England BioLabs) digested pUC-gRNA shuttle vector (Jacobs et al., 2015), with Q5 High-Fidelity DNA Polymerase (New England BioLabs) and primers (Sigma) listed in Table S2. The p201N-Cas9 (Addgene 59175) and pUC-gRNA (Addgene 47024) plasmids were both gifts from Wayne Parrott. Two pairs of oligos (Sigma) corresponding to the consensus gRNA target site in exon two of *MYB186* (Potri.008G089200), *MYB138* (Potri.008G089700) and *MYB38* (Potri.010G165700) were assembled with p201N-Cas9. The NEBuilder HiFi DNA Assembly Cloning Kit (New England Biolobs) was used to assemble p201N-Cas9, *Mt*U6.6 promoter and scaffold fragments with a pair of oligos containing the gRNA target sequence (Table S2). Following transformation into DH5α *E. coli* (Zymo Research Mix & Go! Competent Cells), PCR-positive colonies were used for plasmid purification before Sanger sequencing (Eurofins) confirmation. Plasmids were then heat-shocked into *Agrobacterium tumefaciens* strain C58/GV3101 (pMP90) (Koncz and Schell, 1986) and confirmed by colony PCR.

Populus tremula x *alba* (IRNA 717-1B4) transformation and regeneration was performed as outlined in Meilan and Ma (2006), except 0.05 mg/L 6-benzylaminopurine was used in shoot elongation media, and 200 mg/L L-glutamine was added to all media, with 3 g/L gellan gum (PhytoTechnology Lab) as a gelling agent. Following a 2-day agrobacterial cocultivation, leaf discs were washed in sterile water followed by washing in 200 mg/L cefotaxime and 300 mg/L timentin with shaking for 1.5 hr. Transformants were selected on media supplemented with 100 mg/L kanamycin, 200 mg/L cefotaxime and 300 mg/L timentin for callus induction and shoot regeneration and with kanamycin and timentin for shoot elongation and rooting. All cultures were grown and maintained at 22°C under a 16-hr light/8-hr dark photoperiod with Growlite® FPV24 LED (Barron Lighting Group) at ~150 µmol/m^2/s.

Amplicon sequencing determination of mutation spectrums

Newly emerged leaves were excised from individual events in tissue culture for genomic DNA extraction (Dellaporta et al., 1983). The DNA pellet was resuspended in water with RNase A (10 µg/mL) for amplicon library preparation using GoTaq G2 Green Master Mix (Promega) and primers (Table S2) spanning the gRNA target site (between 264 bp to 280 bp). Samples were then barcoded with Illumina amplicon indexing primers and pooled for Illumina MiSeq nano PE150 sequencing performed at the University of Georgia's Georgia Genomics and Bioinformatics Core. Demultiplexed sequence reads were analyzed by the AGEseq (Analysis of Genome Editing by Sequencing) program (Xue and Tsai, 2015), with mismatch allowance set at 1%, followed by manual curation.

Because initial amplicon data analysis revealed lower editing efficiencies (<90%) than we typically observed in 717 (Zhou et al., 2015; Bewg et al., 2018) at several target sites, we performed *de novo* assembly of WT amplicon reads using Geneious, and recovered seven distinct alleles. We then searched the JGI draft 717 genome assembly v1.0 with the *P. trichocarpa* Nisqually-1 v3.0 (Phytozome v12) *MYB186*, *MYB138* and *MYB38* gene models and extracted the surrounding 50-150 Kb regions from Chr8 and Chr10 for manual annotation against the *P. trichocarpa* Nisqually-1 reference (Figure 3A). The matching *MYB* gene sequences were extracted for error correction using 717 resequencing data (Xue et al., 2015). Curated sequences were used for new (amplicon and allele-/gene-specific) primer design and as references in amplicon data analysis. In the case of WT and transgenic controls with no editing, erroneous read assignments—and hence indel calls—still remained because the amplicon region between some alleles differs only in the number of intronic dinucleotide (GT) repeats (Dataset S1). Misassigned reads led to erroneous indel calls of -2, +2 or their multiples outside of the gRNA target site. For this reason, WT and control samples were processed by ustacks from Stacks 2.3 (Catchen et al., 2011). Parameters were adjusted to avoid collapsing reads with SNPs and/or Indels from paralogous alleles into the same tag group and gapped alignments were disabled. Tags from the output were then used for allele assignment.

Phenotypic and transpiration measurements

Tissue culture plants were transferred into soil (Moisture Control Potting Mix, Scotts Miracle-Grow) in 4" pots and maintained in a walk-in growth room. A subset of plants, 8-10 weeks of age, were transferred to a glasshouse in the Whitehall Forest at the University of Georgia in early summer. Plants were repotted into 1-gal pots and acclimated for two weeks prior to commencing growth measurements. No supplemental lighting was used, and glasshouse temperature was maintained at ~5°C below daytime

ambient temperature by evaporative cooling. Biocontrol (Evergreen Growers Supply) was applied monthly. Plant height and stem diameter measurements were monitored over a 7-week period. Plants were then destructively harvested for stem (30 cm above soil level) and leaf biomass following drying at room temperature in open paper bags for five weeks. To determine rate of water loss during leaf drying, leaf plastochron index LPI-6 and LPI-20 (including petiole) from glasshouse plants were placed on wet paper towel in the dark for 1.5 hr to fully hydrate before being blotted dry with paper towel and allowed to dry abaxial side up at room temperature. Leaf weights were recorded every 20 min. Leaf water uptake via transpiration was performed using whole leaves of growth chamber plants between LPI-10 and LPI-15 matched by size. Leaves were placed on wet paper towel for 1.5 hr in the dark to fully hydrate, and the end of the petiole was trimmed underwater to minimize embolism before placing the leaves, petiole first, into a 15 mL centrifuge tube filled with water. Leaves were then incubated under growth lights (250-300 $\mu M/m^2/s$) and weights were recorded hourly for six hours. An empty tube with water was weighed as evaporation control. A second experiment was performed using trimmed leaves from growth chamber plants using the same methods as above, except leaves were trimmed following a stencil the day before experiment to control for leaf area. All repeated measures ANOVA analyses were performed with JMP Pro Version 15.0.0 (SAS), with *p* values determined after application of the Greenhouse-Geisser epsilon correction. For pest susceptibility monitoring, newly transplanted and acclimated plants were grown in a walk-in growth chamber without regular biocontrol applications. Thrip damage to new growth was then photographed.

RNA-seq analysis

LPI-6 from 10-week-old soil-grown growth chamber plants (three WT, three ΔG and five KO lines) were harvested for RNA extraction using Direct-zol RNA MiniPrep kit (Zymo Research) with Plant RNA Purification Reagent (Invitrogen). For developmental profiling, LPI-1, LPI-5 and LPI-15 were collected from three greenhouse-grown WT plants (~5 ft in height) for RNA extraction as above. RNA-seq library preparation and Illumina NextSeq 500 sequencing was performed at the Georgia Genomics and Bioinformatics Core. We obtained 9.3-15.2 million (M) SE-75 reads per sample for the KO leaf transcriptome experiment, and 10.8-13.3 PE75 reads per sample for the leaf developmental series. After pre-processing to remove adapter and rRNA sequences, reads were mapped to the 717 SNP-substituted genome sPta717 v2 (Xue et al., 2015) using STAR v2.5.3a (Dobin and Gingeras, 2015). Transcript abundance was estimated by featureCounts v1.5.2 (Liao et al., 2014) for differential expression analysis by DESeq2 v1.22 (Love et al., 2014) with multiple testing corrections by SLIM (Wang et al., 2011).

Differentially expressed genes selected based on RPKM (reads per kb transcript per million mapped reads) ≥3, $P \leq 0.01$ and fold-change (FC) ≥1.5 were subjected to Gene Ontology (GO) enrichment analysis using topGO v2.38 (Alexa and Rahnenfuhrer, 2010) with Fisher's exact test and the negative $\log_{10}$-transformed *P* values were used for heatmap visualization. Gene expression ratios between KO and control (WT and ΔG) samples are visualized as heatmaps using BAR HeatMapper Plus Tool (http://bar.utoronto.ca/ntools/cgi-bin/ntools_heatmapper_plus.cgi). Whole-genome duplication inference was determined based on K_s (synonymous substitution rate) distribution and collinearity analysis using the *P. trichocarpa* Nisqually-1 v3.0 reference genome (Phytozome v12) (Tuskan et al., 2006) and the wgd tool suite (Zwaenepoel and Van de Peer, 2018).

Determination of leaf and cuticle wax compositions

One-inch leaf punches were taken from mature leaves of similar size (between LPI-10 and LPI-15) of soil-grown plants in a growth chamber and washed in 4 mL of methylene chloride for 30 sec. The washes were dried under a continuous N_2 stream before resuspension in 400 µL chloroform. A 200µL aliquot was subsequently dried under vacuum and the residues shipped to the Oak Ridge National Laboratory for analysis. Sorbitol (1 mg/mL) was added to the residues as an internal standard and re-dried under N_2. For whole leaf analysis, liquid nitrogen-ground and freeze-dried powders from LPI-5 (25 mg) of control and KO plants were extracted by 80% ethanol to which sorbitol (1 mg/mL) was added and dried under N_2. The samples were derivatized prior to analysis on an Agilent Technologies 7890A GC coupled to a 5975C inert XL MS fitted with an Rtx-5MS capillary column with a 5m Integra-Guard column (Restek) as described in Holwerda et al. (2014). Compound identification was based on mass spectral fragmentation patterns against the NIST08 database and an in-house library built with authentic standards.

Determination of relative anthocyanin content after light-stress

Plants were grown under 16-hr high-light provided by a King Plus 1500W LED full spectrum grow light (KingLED) for four weeks in a growth chamber before leaves (petiole and midvein removed) were harvested and snap frozen in liquid nitrogen. At the time of harvest, plants were experiencing a light intensity gradient of 2300 to 800 µM/m^2/s at LPI-1, depending on the plant height, and of 1-18 µM/m^2/s at LPI-20. Relative anthocyanin content was determined in LPI-3, 5 and 15 following the methods of Neff and Chory (1998) with the following modifications. Briefly, 40 mg of liquid nitrogen-ground and freeze-dried powder were extracted in 800 µL methanol acidified with 1% HCl overnight at 4°C in dark. Supernatant was extracted with 200 µL dH_2O/500 µL chloroform three times before 400 µL was mixed

with 400 µL of 60% acidified methanol for spectrophotometry at A_{530} and A_{657}. Relative abundance of anthocyanin was expressed as A_{530} corrected for scattering at A_{657}. Two-tailed Student's *t*-test was determined using JMP Pro Version 15.0.0 (SAS).

Tissue Imaging and SEM analysis

Images of poplar were taken with either a Google Pixel 3a running Android v11, or a Leica M165 FC dissection microscope attached to a Leica DFC500 camera running Leica Application Suite software v3.8.0. Scanning electron microscopic (SEM) observations were obtained using Hitachi 3400 NII (Hitachi High Technologies America) microscope following optimized protocols at the Center for Ultrastructural Research at the Fort Valley State University. LPI-1 from growth chamber plants or young leaves of tissue culture plants were processed for primary fixation at 25°C in 2 % glutaraldehyde (Electron Microscopy Sciences, EMS) prepared with Sorensen's Phosphate buffer, pH 7.2 (EMS) for one hour and then washed three times for 15 min each with the same buffer before secondary fixation in 1% osmium tetroxide (EMS) prepared in Sorensen's Phosphate buffer, pH 7.2 for 1 hour at 25°C. After three washes with dH_2O for 15 min each, fixed tissues were dehydrated with ethanol series passing through 25%, 50%, 75%, and 95% for 15 min each, followed by three changes of 100% ethanol for 15 min each. Critical point drying of fixed samples was conducted using a critical point dryer (Leica) and then samples were placed on Hitachi M4 aluminum specimen mounts (Ted Pella) using double sided carbon adhesive tabs (EMS) for coating. Gold coating of 50 Å thickness was done for 60 sec using sputter coater (Denton Desk V) under a vacuum pressure of 0.05 torr. Image acquisition in various magnification was done at accelerating voltage of 5 KV.

ACCESSION NUMBERS

The RNA-seq data has been deposited to the National Center for Biotechnology Information's Sequence Read Archive under accession Nos. PRJNA752367 and PRJNA753499.

ACKNOWLEDGEMENTS

The authors thank Gilles Pilate of the Institut National de la Recherche Agronomique, France for providing poplar clone INRA 717-1B4, Margot Chen for tissue culture assistance, Kavita Aulakh for RNA extraction, Yingying Zhu for RNA from developmentally staged leaves and Liang-Jiao Xue for guidance on RNA-seq data processing. We additionally thank the Department of Energy Joint Genome Institute and

collaborators for prepublication access to the *Populus tremula* x *P. alba* (IRNA 717-1B4) genome sequence and annotation.

SUPPORTING INFORMATION

Table S1. Transcript levels of trichome-regulating MBW genes based on RNA-seq.

Table S2. Primers used in this study.

Figure S1. PCR confirmation of NA alleles using allele-specific primers.

Figure S2. Sequence alignment of wild type and fusion *MYB* alleles from KO-5 and KO-69.

Figure S3. Susceptibility of trichomeless mutants to thrip damage.

Dataset S1. CRISPR/Cas9 mutation patterns of the eight target MYB alleles in ΔG and KO lines.

Dataset S2. Differentially expressed genes detected in trichomeless leaves.

FIGURE LEGENDS

Figure 1. Expression of clade 15 *MYB* transcription factors during *Populus* leaf maturation.
A simplified phylogenetic tree is shown with duplication history noted on the left. Data are mean±SD of n=3. LPI, leaf plastochron index; FPKM, fragments per kilobase of transcript per million mapped reads; MYB186, Potri.008G089200; MYB138, Potri.008G089700; MYB38, Potri.010G165700; and MYB83, Potri.017G086300.

Figure 2. CRISPR/Cas9 KO of trichome-regulating *MYBs*.
A, Schematic illustrations of the *MYB* gene structure, gRNA target site, and base pairing between the genomic target (black) and the gRNA spacer (red)-scaffold (blue) molecule. Black line denotes the protospacer adjacent motif (PAM). **B**, Zoomed-in view of the ΔG vector configuration at the gRNA spacer-scaffold junction with a guanine omission. **C**-**R**, Representative shoot tip (C, G, K, O) and LPI-1 abaxial (D, H, L, P) phenotypes and SEM images (E, F, I, J, M, N, Q, R) of soil-grown WT (D, E), Cas9 vector control (C), ΔG control (G-I), KO-27 (K-M), and null mutant (O-Q) plants, and leaf abaxial (F, N) or adaxial (J, R) images of tissue cultured ΔG (F, J) and null mutant (N, R) plants. Scale bar = 3 mm (D, H, L, P), 500 μm (E, I, M), 1 mm (Q), or 25 μm (F, J, N, R).

606 **Figure 3.** Mutation analysis of trichomeless mutants.

607 **A**, Schematic illustration of *MYB186* and *MYB138* on Chr8 subgenomes (main and alternative, or Chr8m
608 and Chr8a, respectively) and *MYB38* on Chr10m and Chr10a of the 717 genome. Neighboring genes are
609 color coded for synteny and the putative duplication block containing *MYB186* and *MYB138* on Chr8 is
610 marked by red brackets. Black triangles denote the eight gRNA target sites. **B**, Mutation spectrum
611 determined by amplicon sequencing. The eight alleles are arranged by genomic position for each plant
612 line and color-coded for the editing outcomes: green, unedited (intact); orange, indel; and grey, no
613 amplification (NA). **C**, Pie chart summary of the overall (left) and indel (right) editing patterns. **D**, PCR
614 amplification of the six *MYB* alleles on Chr8 from two WT, one ΔG and four KO lines. The four KO lines
615 were selected to represent one (KO-5 and KO-69) or two (KO-63 and KO-70) remaining Chr08 alleles.
616 *UBC* (*ubiquitin-conjugating enzyme*) was included as loading control. M, molecular weight marker; ntc,
617 no-template control. **E**, Sanger sequencing of PCR products from D. Sequence alignment of the six alleles
618 flanking the gRNA target site (red) is shown on top and chromatograms of the same region are shown
619 below. Grey shaded regions are introns and PAM is underlined and boxed in blue for correspondence
620 with the sequence traces below. Black triangles denote the Cas9 cleavage site and black dashed box
621 corresponds to the 2-bp deletion (-2) detected in KO-5 and KO-69. The two fusion alleles as determined
622 by SNPs are marked below the KO-5 and KO-69 traces (see Supplemental Figure S2 for the full sequence
623 alignment).
624
625 **Figure 4.** Phenotypic characterization of trichomeless KO mutants.
626 **A-B**, Height (A) and diameter (B) growth monitored over seven weeks. **C**-**D**, Stem (C) and leaf (D)
627 biomass at harvest. Only LPI31-LPI40 were used for leaf biomass. **E**, Transpiration-driven water uptake of
628 size-matched whole leaves or leaves trimmed with stencil to control for surface area. **F**, Water loss
629 during drying of leaves LPI-6 and LPI-20. Data are mean ± SD of n=5-7 controls (WT and transgenic
630 controls) or KO mutants grown in a greenhouse (A-D, F) or in a growth chamber (E). *P* values were
631 determined using repeated measures ANOVA (A-B, E-F) or 2-tailed *t*-test (C-D).
632
633 **Figure 5.** Transcriptional responses of trichomeless leaves.
634 **A**, Expression response heatmaps of genes involved in trichome development, biosynthesis and signaling
635 of GA and JA signaling and morphogenesis. B, Gene Ontology (GO) enrichment analysis of genes
636 differentially up- or down-regulated in trichomeless leaves related to the control. Representative GO
637 terms are visualized by the negative $\log_{10}$-transformed *P* values, with the color scales shown at the

bottom. Boldfaced values indicate *P*<0.05). C, Expression heatmaps of genes involved in regulation of circadian rhythm and light responses. Expression responses in A and C are shown in log_2-transformed fold-change (FC, mutant/control) and visualized according to the color scales at the bottom. Average basal expression levels from control samples are shown in RPKM (reads per kilobase of transcript per million mapped reads) and visualized according to the color scales at the bottom.

Figure 6. Anthocyanin accumulation under high light conditions.
A-**B**, Representative examples of LPI-1 to LPI-5 from a Cas9 vector control plant (A) or a trichomeless mutant (B). **C**, Anthocyanin contents of LPI-3, LPI-5 and LPI-15. Data are mean±SE of n=6 control or n=10 KO plants. *P* values were determined using 2-tailed *t*-test.

Figure 7. Cuticular wax composition of trichomeless and control leaves.
A, Total wax load. **B**, Major classes of cuticular wax. **C**, Fatty alcohols (C26, 1-hexacosanol; C28, 1-octacosanol) in wax (left) or whole leaves (right). **D**, β-sitosterol detected in wax (left) or whole leaves (right). **E**, Triterpenes detected in wax (top) or whole leaves (bottom). Ergosterone, 14,24-dimethyl-ergosta-8,25-dien-3-one; cycloartanone, 24-methylene cycloartan-3-one; lanosterone, lanosta-8,24-dien-3-one. Data are mean±SD of n=5. All concentration estimates were based on sorbitol equivalent. Statistical significance was determined by 2-tailed *t*-test (* *P*<0.05, ** *P*<0.01, *** *P*<0.001). nd, not detected. **F**, Expression response heatmaps of genes involved in fatty acid and wax biosynthesis. Data presentation is the same as in Figure 5.

REFERENCES

Alexa A, Rahnenfuhrer J (2010) topGO: Enrichment Analysis for Gene Ontology. R package version 2.0.
Bewg WP, Ci D, Tsai CJ (2018) Genome editing in trees: From multiple repair pathways to long-term stability. Frontiers in Plant Science **9:** 1732
Bickford CP (2016) Ecophysiology of leaf trichomes. Functional Plant Biology **43:** 807-814
Briggs WR, Beck CF, Cashmore AR, Christie JM, Hughes J, Jarillo JA, Kagawa T, Kanegae H, Liscum E, Nagatani A, Okada K, Salomon M, Rüdiger W, Sakai T, Takano M, Wada M, Watson JC (2001) The phototropin family of photoreceptors. Plant Cell **13:** 993-997
Catchen JM, Amores A, Hohenlohe P, Cresko W, Postlethwait JH (2011) Stacks: Building and genotyping loci *de novo* from short-read sequences. Genes Genomes Genetics **1:** 171-182
Cheng Y, Wang L, Abbas M, Huang X, Wang Q, Wu A, Wei H, Peng S, Dai X, Li Q (2021) MicroRNA319-mediated gene regulatory network impacts leaf development and morphogenesis in poplar. Forestry Research **1:** 4

673 **Dellaporta SL, Wood J, Hicks JB** (1983) A plant DNA minipreparation: Version II. Plant Molecular Biology
674 Reporter **1:** 19-21
675 **Dobin A, Gingeras TR** (2015) Mapping RNA-seq reads with STAR. Curr Protoc Bioinformatics **51:**
676 11.14.11-11.14.19
677 **dos Santos Tozin LR, de Melo Silva SC, Rodrigues TM** (2016) Non-glandular trichomes in Lamiaceae and
678 Verbenaceae species: Morphological and histochemical features indicate more than physical
679 protection. New Zealand Journal of Botany **54:** 446-457
680 **Downes BP, Stupar RM, Gingerich DJ, Vierstra RD** (2003) The HECT ubiquitin-protein ligase (UPL) family
681 in *Arabidopsis*: UPL3 has a specific role in trichome development. Plant Journal **35:** 729-742
682 **Falginella L, Andre CM, Legay S, Lin-Wang K, Dare AP, Deng C, Rebstock R, Plunkett BJ, Guo L, Cipriani**
683 **G, Espley RV** (2021) Differential regulation of triterpene biosynthesis induced by an early failure
684 in cuticle formation in apple. Horticulture Research **8:** 75
685 **Fambrini M, Pugliesi C** (2019) The dynamic genetic-hormonal regulatory network controlling the
686 trichome development in leaves. Plants **8:** 253
687 **Filichkin SA, Breton G, Priest HD, Dharmawardhana P, Jaiswal P, Fox SE, Michael TP, Chory J, Kay SA,**
688 **Mockler TC** (2011) Global profiling of rice and poplar transcriptomes highlights key conserved
689 circadian-controlled pathways and cis-regulatory modules. PLoS One **6:** e16907
690 **Folkers U, Berger J, Hülskamp M** (1997) Cell morphogenesis of trichomes in *Arabidopsis*: Differential
691 control of primary and secondary branching by branch initiation regulators and cell growth.
692 Development **124:** 3779-3786
693 **Gachotte D, Meens R, Benveniste P** (1995) An *Arabidopsis* mutant deficient in sterol biosynthesis:
694 Heterologous complementation by ERG 3 encoding a Δ7-sterol-C-5-desaturase from yeast. Plant
695 Journal **8:** 407-416
696 **Galletti R, Johnson KL, Scofield S, San-Bento R, Watt AM, Murray JA, Ingram GC** (2015) DEFECTIVE
697 KERNEL 1 promotes and maintains plant epidermal differentiation. Development **142:** 1978-
698 1983
699 **Gan Y, Kumimoto R, Liu C, Ratcliffe O, Yu H, Broun P** (2006) GLABROUS INFLORESCENCE STEMS
700 modulates the regulation by gibberellins of epidermal differentiation and shoot maturation in
701 Arabidopsis. Plant Cell **18:** 1383-1395
702 **Gilding EK, Marks MD** (2010) Analysis of purified *glabra3-shapeshifter* trichomes reveals a role for
703 *NOECK* in regulating early trichome morphogenic events. Plant Journal **64:** 304-317
704 **Glover BJ, Perez-Rodriguez M, Martin C** (1998) Development of several epidermal cell types can be
705 specified by the same MYB-related plant transcription factor. Development **125:** 3497-3508
706 **Hall A, Bastow RM, Davis SJ, Hanano S, McWatters HG, Hibberd V, Doyle MR, Sung S, Halliday KJ,**
707 **Amasino RM, Millar AJ** (2003) The TIME FOR COFFEE gene maintains the amplitude and timing
708 of Arabidopsis circadian clocks. Plant Cell **15:** 2719-2729
709 **Hamaguchi A, Yamashino T, Koizumi N, Kiba T, Kojima M, Sakakibara H, Mizuno T** (2008) A small
710 subfamily of Arabidopsis RADIALIS-LIKE SANT/MYB genes: A link to HOOKLESS1-mediated signal
711 transduction during early morphogenesis. Bioscience, Biotechnology, and Biochemistry **72:**
712 2687-2696
713 **Hegebarth D, Buschhaus C, Wu M, Bird D, Jetter R** (2016) The composition of surface wax on trichomes
714 of *Arabidopsis thaliana* differs from wax on other epidermal cells. Plant Journal **88:** 762-774
715 **Holwerda EK, Thorne PG, Olson DG, Amador-Noguez D, Engle NL, Tschaplinski TJ, van Dijken JP, Lynd**
716 **LR** (2014) The exometabolome of *Clostridium thermocellum* reveals overflow metabolism at high
717 cellulose loading. Biotechnology for Biofuels **7:** 155
718 **Hülskamp M** (2004) Plant trichomes: A model for cell differentiation. Nature Reviews: Molecular Cell
719 Biology **5:** 471-480

Imaizumi T, Tran HG, Swartz TE, Briggs WR, Kay SA (2003) FKF1 is essential for photoperiodic-specific light signalling in *Arabidopsis*. Nature **426:** 302-306

Jacobs TB, LaFayette PR, Schmitz RJ, Parrott WA (2015) Targeted genome modifications in soybean with CRISPR/Cas9. BMC Biotechnology **15:** 16

Jakoby MJ, Falkenhan D, Mader MT, Brininstool G, Wischnitzki E, Platz N, Hudson A, Hulskamp M, Larkin J, Schnittger A (2008) Transcriptional profiling of mature Arabidopsis trichomes reveals that *NOECK* encodes the MIXTA-like transcriptional regulator MYB106. Plant Physiology **148:** 1583-1602

Jones MA, Covington MF, DiTacchio L, Vollmers C, Panda S, Harmer SL (2010) Jumonji domain protein JMJD5 functions in both the plant and human circadian systems. Proc Natl Acad Sci U S A **107:** 21623-21628

Karabourniotis G, Liakopoulos G, Nikolopoulos D, Bresta P (2020) Protective and defensive roles of non-glandular trichomes against multiple stresses: Structure–function coordination. Journal of Forestry Research **31:** 1-12

Koncz C, Schell J (1986) The promoter of TL-DNA gene *5* controls the tissue-specific expression of chimaeric genes carried by a novel type of *Agrobacterium* binary vector. Molecular & General Genetics **204:** 383-396

Lange BM, Srividya N (2019) Enzymology of monoterpene functionalization in glandular trichomes. Journal of Experimental Botany **70:** 1095-1108

Lange BM, Turner GW (2013) Terpenoid biosynthesis in trichomes - Current status and future opportunities. Plant Biotechnology Journal **11:** 2-22

Larkin JC, Brown ML, Schiefelbein J (2003) How do cells know what they want to be when they grow up? Lessons from epidermal patterning in Arabidopsis. Annual Review of Plant Biology **54:** 403-430

Liakopoulos G, Nikolopoulos D, Klouvatou A, Vekkos KA, Manetas Y, Karabourniotis G (2006) The photoprotective role of epidermal anthocyanins and surface pubescence in young leaves of grapevine (Vitis vinifera). Annals of Botany **98:** 257-265

Liao Y, Smyth GK, Shi W (2014) featureCounts: an efficient general purpose program for assigning sequence reads to genomic features. Bioinformatics **30:** 923-930

Long JA, Ohno C, Smith ZR, Meyerowitz EM (2006) TOPLESS regulates apical embryonic fate in Arabidopsis. Science **312:** 1520-1523

Love M, Huber W, Anders S (2014) Moderated estimation of fold change and dispersion for RNA-seq data with DESeq2. Genome Biology **15:** 550

Machado A, Wu Y, Yang Y, Llewellyn DJ, Dennis ES (2009) The MYB transcription factor GhMYB25 regulates early fibre and trichome development. The Plant Journal **59:** 52-62

Maes L, Goossens A (2010) Hormone-mediated promotion of trichome initiation in plants is conserved but utilizes species- and trichome-specific regulatory mechanisms. Plant Signaling & Behavior **5:** 205-207

Maes L, Inzé D, Goossens A (2008) Functional specialization of the TRANSPARENT TESTA GLABRA1 network allows differential hormonal control of laminal and marginal trichome initiation in *Arabidopsis* rosette leaves. Plant Physiol **148:** 1453-1464

Matías-Hernández L, Aguilar-Jaramillo AE, Cigliano RA, Sanseverino W, Pelaz S (2016) Flowering and trichome development share hormonal and transcription factor regulation. Journal of Experimental Botany **67:** 1209-1219

Matsushika A, Makino S, Kojima M, Mizuno T (2000) Circadian waves of expression of the APRR1/TOC1 family of pseudo-response regulators in *Arabidopsis thaliana:* Insight into the plant circadian clock. Plant Cell Physiology **41:** 1002-1012

Mauriat M, Moritz T (2009) Analyses of GA20ox- and GID1-over-expressing aspen suggest that gibberellins play two distinct roles in wood formation. Plant Journal **58:** 989-1003

Meilan R, Ma C (2006) Poplar (*Populus* spp.). *In* K Wang, ed, Agrobacterium Protocols Volume 2. Methods in Molecular Biology, Vol 344. Humana Press, Totowa, NJ

Narita NN, Moore S, Horiguchi G, Kubo M, Demura T, Fukuda H, Goodrich J, Tsukaya H (2004) Overexpression of a novel small peptide ROTUNDIFOLIA4 decreases cell proliferation and alters leaf shape in *Arabidopsis thaliana*. Plant Journal **38:** 699-713

Neff MM, Chory J (1998) Genetic interactions between Phytochrome A, Phytochrome B, and Cryptochrome 1 during Arabidopsis development. Plant Physiology **118:** 27-36

Ni M (2005) Integration of light signaling with photoperiodic flowering and circadian rhythm. Cell Research **15:** 559-566

Oppenheimer DG, Pollock MA, Vacik J, Szymanski DB, Ericson B, Feldmann K, Marks MD (1997) Essential role of a kinesin-like protein in Arabidopsis trichome morphogenesis. Proceedings of the National Academy of Sciences of the United States of America **94:** 6261-6266

Oshima Y, Shikata M, Koyama T, Ohtsubo N, Mitsuda N, Ohme-Takagi M (2013) MIXTA-like transcription factors and WAX INDUCER1/SHINE1 coordinately regulate cuticle development in *Arabidopsis* and *Torenia fournieri*. Plant Cell **25:** 1609-1624

Park DH, Somers DE, Kim YS, Choy YH, Lim HK, Soh MS, Kim HJ, Kay SA, Nam HG (1999) Control of circadian rhythms and photoperiodic flowering by the Arabidopsis GIGANTEA gene. Science **285:** 1579-1582

Payne WW (1978) A glossary of plant hair terminology. Brittonia **30:** 239-255

Plett JM, Wilkins O, Campbell MM, Ralph SG, Regan S (2010) Endogenous overexpression of *Populus MYB186* increases trichome density, improves insect pest resistance, and impacts plant growth. Plant Journal **64:** 419-432

Qi T, Song S, Ren Q, Wu D, Huang H, Chen Y, Fan M, Peng W, Ren C, Xie D (2011) The Jasmonate-ZIM-domain proteins interact with the WD-Repeat/bHLH/MYB complexes to regulate jasmonate-mediated anthocyanin accumulation and trichome initiation in *Arabidopsis thaliana*. Plant Cell **23:** 1795-1814

Qiu JL, Jilk R, Marks MD, Szymanski DB (2002) The Arabidopsis SPIKE1 gene is required for normal cell shape control and tissue development. Plant Cell **14:** 101-118

Ramsay NA, Glover BJ (2005) MYB-bHLH-WD40 protein complex and the evolution of cellular diversity. Trends in Plant Science **10:** 63-70

Reddy VS, Day IS, Thomas T, Reddy AS (2004) KIC, a novel Ca2+ binding protein with one EF-hand motif, interacts with a microtubule motor protein and regulates trichome morphogenesis. Plant Cell **16:** 185-200

Rowland O, Zheng H, Hepworth SR, Lam P, Jetter R, Kunst L (2006) CER4 encodes an alcohol-forming fatty acyl-coenzyme A reductase involved in cuticular wax production in Arabidopsis. Plant Physiology **142:** 866-877

Schuepp PH (1993) Leaf boundary layers. New Phytologist **125:** 477-507

Schuurink R, Tissier A (2020) Glandular trichomes: Micro-organs with model status? New Phytologist **225:** 2251-2266

Smillie RM, Hetherington SE (1999) Photoabatement by anthocyanin shields photosynthetic systems from light stress. Photosynthetica **36:** 451-463

Soetaert SSA, Van Neste CMF, Vandewoestyne ML, Head SR, A. G, Van Nieuwerburgh FCW, Deforce DLD (2013) Differential transcriptome analysis of glandular and filamentous trichomes in *Artemisia annua*. BMC Plant Biology **13:** 220

Soundappan I, Bennett T, Morffy N, Liang Y, Stanga JP, Abbas A, Leyser O, Nelson DC (2015) SMAX1-LIKE/D53 family members enable distinct MAX2-dependent responses to strigolactones and karrikins in Arabidopsis. Plant Cell **27:** 3143-3159

Tao Q, Guo D, Wei B, Zhang F, Pang C, Jiang H, Zhang J, Wei T, Gu H, Qu LJ, Qin G (2013) The TIE1 transcriptional repressor links TCP transcription factors with TOPLESS/TOPLESS-RELATED corepressors and modulates leaf development in Arabidopsis. Plant Cell **25:** 421-437

Thimmappa R, Geisler K, Louveau T, O'Maille P, Osbourn A (2014) Triterpene biosynthesis in plants. Annual Review of Plant Biology **65:** 225-257

Tuskan GA, DiFazio S, Jansson S, Bohlmann J, Grigoriev I, Hellsten U, Putnam N, Ralph S, Rombauts S, Salamov A, Schein J, Sterck L, Aerts A, Bhalerao RR, Bhalerao RP, Blaudez D, Boerjan W, Brun A, Brunner A, Busov V, Campbell M, Carlson J, Chalot M, Chapman J, Chen GL, Cooper D, Coutinho PM, Couturier J, Covert S, Cronk Q, Cunningham R, Davis J, Degroeve S, Dejardin A, dePamphilis C, Detter J, Dirks B, Dubchak I, Duplessis S, Ehlting J, Ellis B, Gendler K, Goodstein D, Gribskov M, Grimwood J, Groover A, Gunter L, Hamberger B, Heinze B, Helariutta Y, Henrissat B, Holligan D, Holt R, Huang W, Islam-Faridi N, Jones S, Jones-Rhoades M, Jorgensen R, Joshi C, Kangasjarvi J, Karlsson J, Kelleher C, Kirkpatrick R, Kirst M, Kohler A, Kalluri U, Larimer F, Leebens-Mack J, Leple JC, Locascio P, Lou Y, Lucas S, Martin F, Montanini B, Napoli C, Nelson DR, Nelson C, Nieminen K, Nilsson O, Pereda V, Peter G, Philippe R, Pilate G, Poliakov A, Razumovskaya J, Richardson P, Rinaldi C, Ritland K, Rouze P, Ryaboy D, Schmutz J, Schrader J, Segerman B, Shin H, Siddiqui A, Sterky F, Terry A, Tsai CJ, Uberbacher E, Unneberg P, Vahala J, Wall K, Wessler S, Yang G, Yin T, Douglas C, Marra M, Sandberg G, Van de Peer Y, Rokhsar D (2006) The genome of black cottonwood, Populus trichocarpa (Torr. & Gray). Science **313:** 1596-1604

Walker AR, Davison PA, Bolognesi-Winfield AC, James CM, Srinivasan N, Blundell TL, Esch JJ, Marks MD, Gray JC (1999) The TRANSPARENT TESTA GLABRA1 locus, which regulates trichome differentiation and anthocyanin biosynthesis in *arabidopsis*, encodes a WD40 repeat protein. Plant Cell **11:** 1337-1349

Wang B, Luo Q, Li Y, Yin L, Zhou N, Li X, Gan J, Dong A (2020) Structural insights into target DNA recognition by R2R3-MYB transcription factors. Nucleic Acids Research **48:** 460-471

Wang H-Q, Tuominen LK, Tsai C-J (2011) SLIM: A sliding linear model for estimating the proportion of true null hypotheses in datasets with dependence structures. Bioinformatics **27:** 225-231

Wang S, Chen J-G (2014) Regulation of cell fate determination by single-repeat R3 MYB transcription factors in Arabidopsis. Frontiers in Plant Science **5**

Wang S, Chen JG (2014) Regulation of cell fate determination by single-repeat R3 MYB transcription factors in Arabidopsis. Frontiers in Plant Science **5:** 133

Wang W, Wang Y, Zhang Q, Qi Y, Guo D (2009) Global characterization of Artemisia annua glandular trichome transcriptome using 454 pyrosequencing. BMC Genomics **10:** 465

Wen J, Lease KA, Walker JC (2004) DVL, a novel class of small polypeptides: Overexpression alters *Arabidopsis* development. Plant Journal **37:** 668-677

Widemann E, Miesch L, Lugan R, Holder E, Heinrich C, Aubert Y, Miesch M, Pinot F, Heitz T (2013) The amidohydrolases IAR3 and ILL6 contribute to jasmonoyl-isoleucine hormone turnover and generate 12-hydroxyjasmonic acid upon wounding in *Arabidopsis* leaves. Journal of Biological Chemistry **288:** 31701-31714

Wilkins O, Nahal H, Foong J, Provart NJ, Campbell MM (2009) Expansion and diversification of the *Populus* R2R3-MYB family of transcription factors. Plant Physiology **149:** 981-993

Xue L-J, Alabady MS, Mohebbi M, Tsai C-J (2015) Exploiting genome variation to improve next-generation sequencing data analysis and genome editing efficiency in Populus tremula x alba 717-1B4. Tree Genetics & Genomes **11:** 82

Xue LJ, Tsai CJ (2015) AGEseq: Analysis of genome editing by sequencing. Molecular Plant **8:** 1428-1430

Zhang B, Hülskamp M (2019) Evolutionary analysis of MBW function by phenotypic rescue in *Arabidopsis thaliana*. Frontiers in Plant Science **10**

Zhang F, Gonzalez A, Zhao M, Payne CT, Lloyd A (2003) A network of redundant bHLH proteins functions in all TTG1-dependent pathways of *Arabidopsis*. Development **130:** 4859-4869

Zhao M, Morohashi K, Hatlestad G, Grotewold E, Lloyd A (2008) The TTG1-bHLH-MYB complex controls trichome cell fate and patterning through direct targeting of regulatory loci. Development **135:** 1991-1999

Zhou X, Jacobs TB, Xue L-J, Harding SA, Tsai C-J (2015) Exploiting SNPs for biallelic CRISPR mutations in the outcrossing woody perennial *Populus* reveals 4-coumarate:CoA ligase specificity and redundancy. New Phytologist **208:** 298-301

Zwaenepoel A, Van de Peer Y (2018) wgd—simple command line tools for the analysis of ancient whole-genome duplications. Bioinformatics **35:** 2153-2155

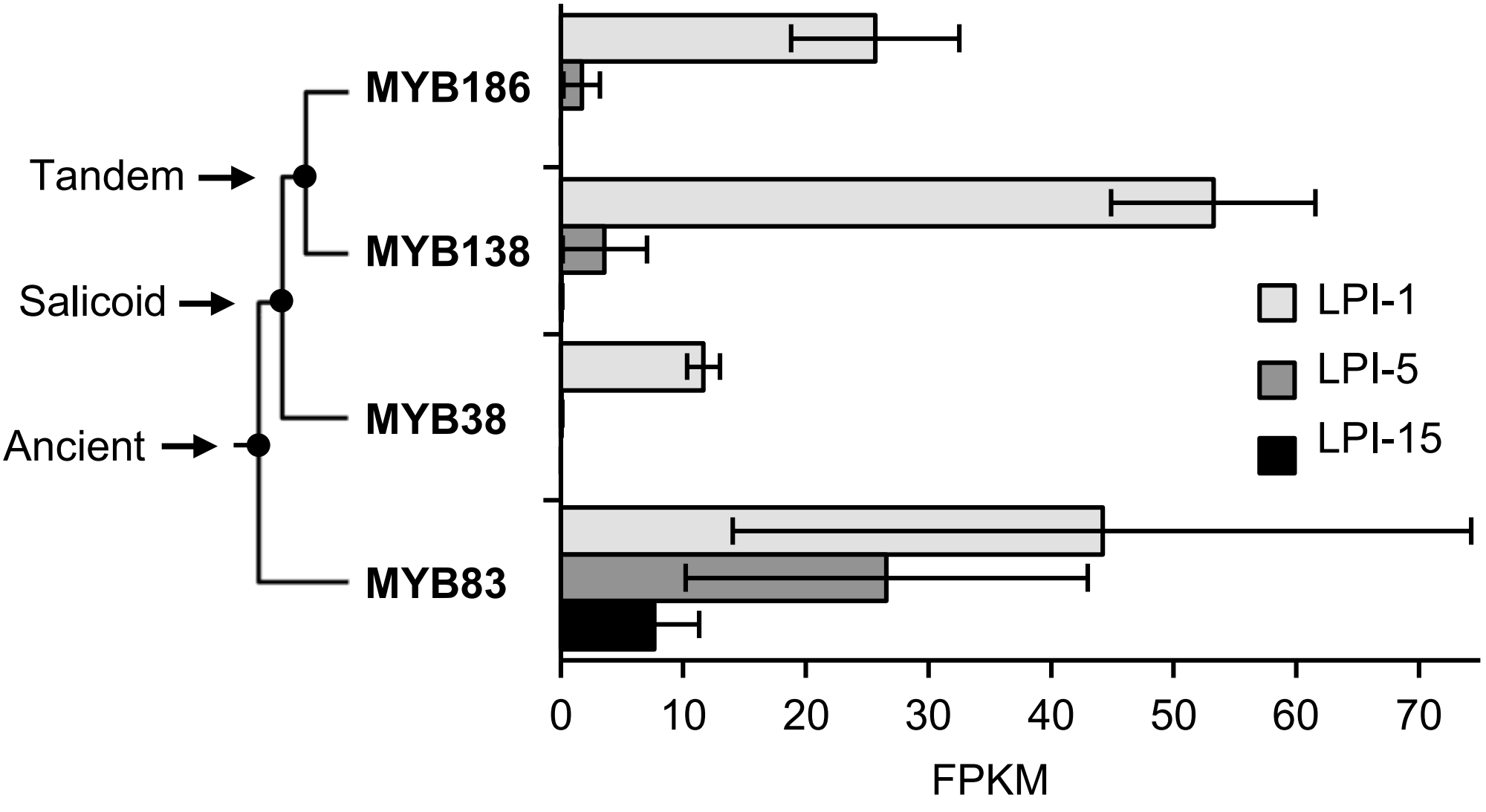

Figure 1. Expression of clade 15 *MYB* transcription factors during *Populus* leaf maturation. A simplified phylogenetic tree is shown with duplication history noted on the left. Data are mean ± SD of n=3. LPI, leaf plastochron index; FPKM, fragments per kilobase of transcript per million mapped reads; MYB186, Potri.008G089200; MYB138, Potri.008G089700; MYB38, Potri.010G165700; and MYB83, Potri.017G086300.

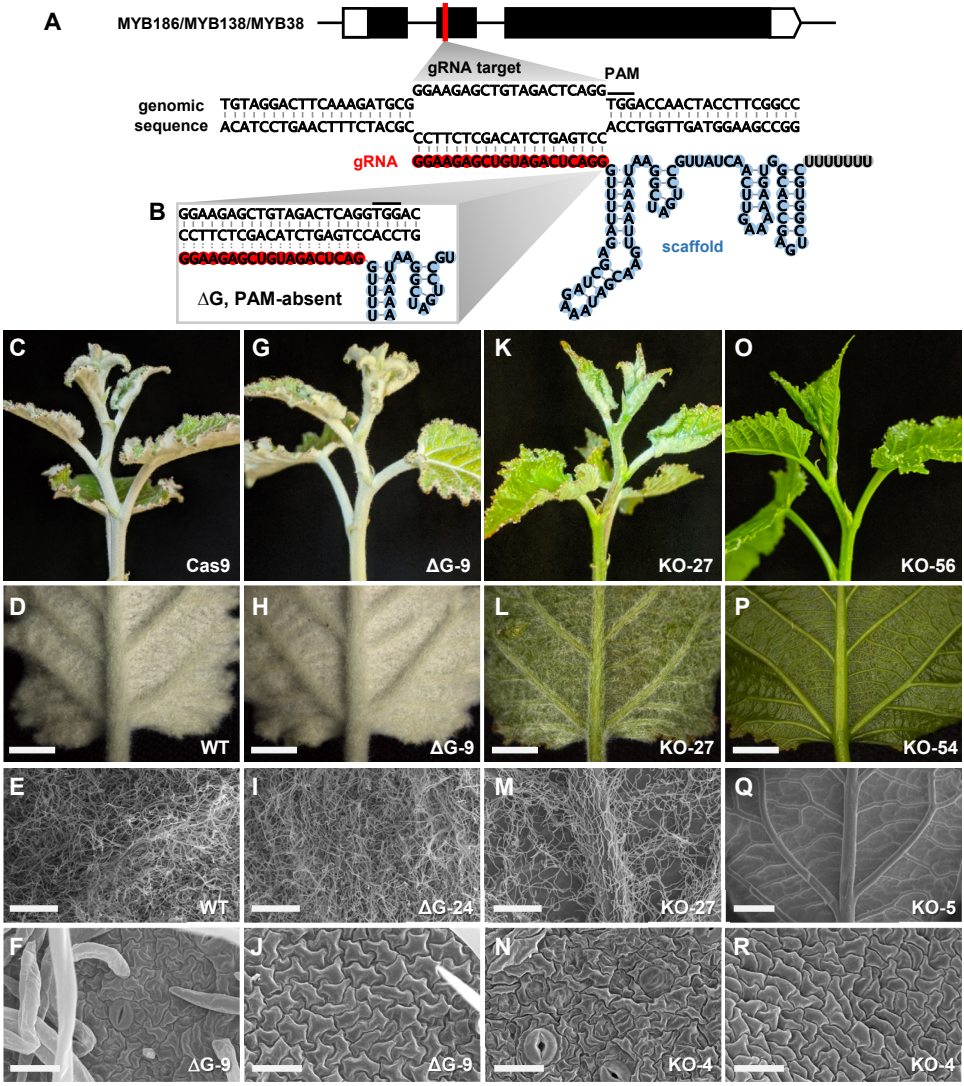

Figure 2. CRISPR/Cas9 KO of trichome-regulating *MYBs*. **A**, Schematic illustrations of the *MYB* gene structure, gRNA target site, and base pairing between the genomic target (black) and the gRNAspacer (red)-scaffold (blue) molecule. Black line denotes the protospacer adjacent motif (PAM). **B**, Zoomed-in view of the ΔG vector configuration at the gRNA spacer-scaffold junction with a guanine omission. **C**-**R**, Representative shoot tip (C, G, K, O) and LPI-1 abaxial (D, H, L, P) phenotypes and SEM images (E, F, I, J, M, N, Q, R) of soil-grown WT (D, E), Cas9 vector control (C), ΔG control (G-I), KO-27 (K-M), and mutant (O-Q) plants, and leaf abaxial (F, N) or adaxial (J, R) images of tissue cultured ΔG (F, J) and mutant (N, R) plants. Scale bar = 3 mm (D, H, L, P), 500 μm (E, I, M), 1 mm (Q), or 25 μm (F, J, N, R).

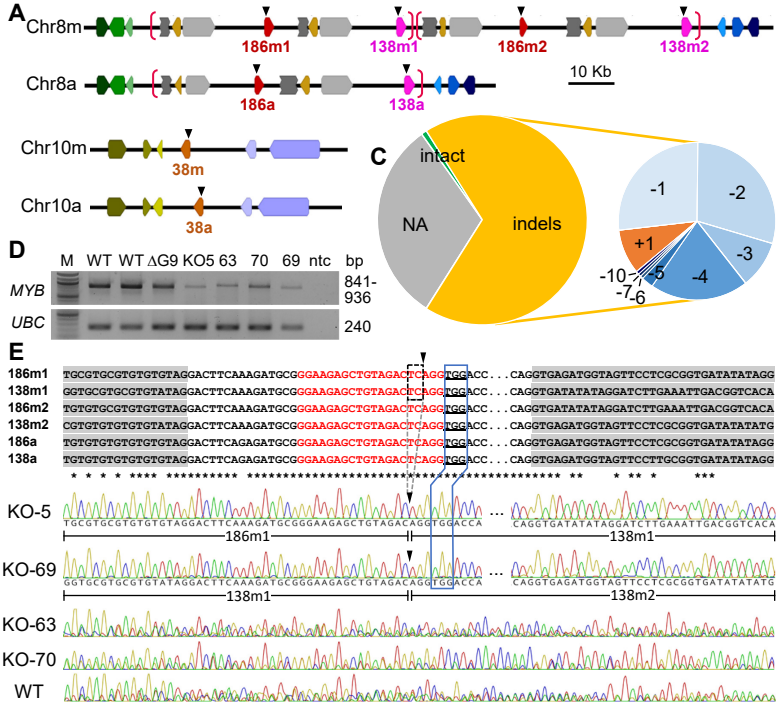

B

	Main Chr8				Alt. Chr8		Chr10	
	186m1	138m1	186m2	138m2	186a	138a	38m	38a
Control								
ΔG								
KO-2	+1	-2			-1		-2	-1
KO-4	-1			-4	-2	-1	-2	+1
KO-5	-2						-4	-1
KO-7	-1	-2			-1	-4	-1	-3
KO-10		-1		-1			-3	-4
KO-12	-1		-1		-10	-3	-7	-2
KO-18		+1			-2		-1	-2
KO-19	-1	-4	-2	-4	-1	-2	-4	-2
KO-22					-2	-1	-2	-4
KO-24				-1	-3	-3	-1	-2
KO-25	-4	-2	-4	-1	-4	-2	-1	-4
KO-26		-3	-3		-4	+1		-2
KO-27	-2	+1	-2	-1	-2	-3		
KO-28	-4	-2	-1	-4	+1	-2	+1	-1
KO-29	+1	-2		-2	-2		-1	-2
KO-30			-2	-6	-4	-4	-1	
KO-33			-2	-4	-1	-3	-2	-1
KO-39	-2	-1			-2	-1	-1	-1
KO-40	-5			-3	+1	+1	-1	-4
KO-44		-1		+1			-1	-1
KO-46	-2	-2	-2	-1	-2	-2	-2	-3
KO-48	-4	-2		-1			-1	-2
KO-54	-1		-1		-2	-3	+1	-4
KO-56			-1	-5	+1	-1		+1
KO-61				-4	-3		-3	-2
KO-62	-4	-4	-4	-1	-2	+1	-2	-2
KO-63					-4	-2		-4
KO-67			-5	-4	-1	-4	-2	-4
KO-69		-2					-5	-3
KO-70	-4				-3		-4	-4

Intact (unedited) indel NA (no amplification)

Figure 3. Mutation analysis of trichomeless mutants. **A**, Schematic illustration of *MYB186* and *MYB138* on Chr8 subgenomes (main and alternative, or Chr8m and Chr8a, respectively) and *MYB38* on Chr10m and Chr10a of the 717 genome. Neighboring genes are color coded for synteny and the putative duplication block containing *MYB186* and *MYB138* on Chr8 is marked by red brackets. Black triangles denote the eight gRNA target sites. **B**, Mutation spectrum determined by amplicon sequencing. The eight alleles are arranged by genomic position for each plant line and color-coded for the editing outcomes: green, unedited (intact); orange, indel; and grey, no amplification (NA). **C**, Pie chart summary of the overall (left) and indel (right) editing patterns. **D**, PCR amplification of the six *MYB* alleles on Chr8 from two WT, one ΔG and four KO lines. The four KO lines were selected to represent one (KO-5 and KO-69) or two (KO-63 and KO-70) remaining Chr08 alleles. *UBC* (ubiquitin-conjugating enzyme) was included as loading control. M, molecular weight marker; ntc, no-template control. **E**, Sanger sequencing of PCR products from D. Sequence alignment of the six alleles flanking the gRNA target site (red) is shown on top and chromatograms of the same region are shown below. Grey shaded regions are introns and PAM is underlined and boxed in blue for correspondence with the sequence traces below. Black triangles denote the Cas9 cleavage site and black dashed box corresponds to the 2-bp deletion (-2) detected in KO-5 and KO-69. The two fusion alleles as determined by SNPs are marked below the KO-5 and KO-69 traces (see Supplemental Figure S2 for the full sequence alignment).

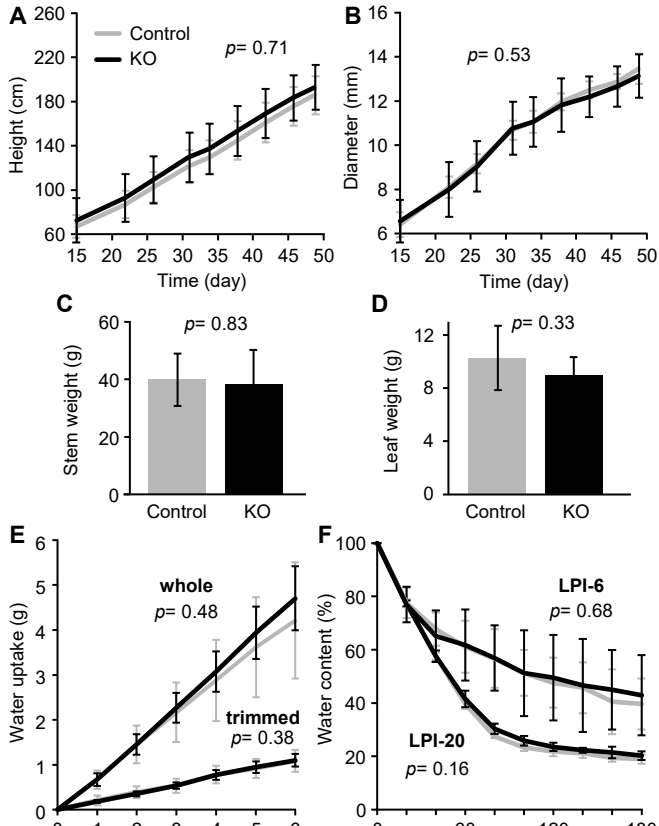

Figure 4. Phenotypic characterization of trichomeless KO mutants. **A-B**, Height (A) and diameter (B) growth monitored over seven weeks. **C-D**, Stem (C) and leaf (D) biomass at harvest. Only LPI31-LPI40 were used for leaf biomass. **E**, Transpiration-driven water uptake of size-matched whole leaves or leaves trimmed with stencil to control for surface area. **F**, Water loss during drying of leaves LPI-6 and LPI-20. Data are mean ± SD of n=5-7 controls (WT and transgenic controls) or KO mutants grown in a greenhouse (A-D, F) or in a growth chamber (E). *P* values were determined using repeated measures ANOVA (A-B, E-F) or 2-tailed *t*-test (C-D).

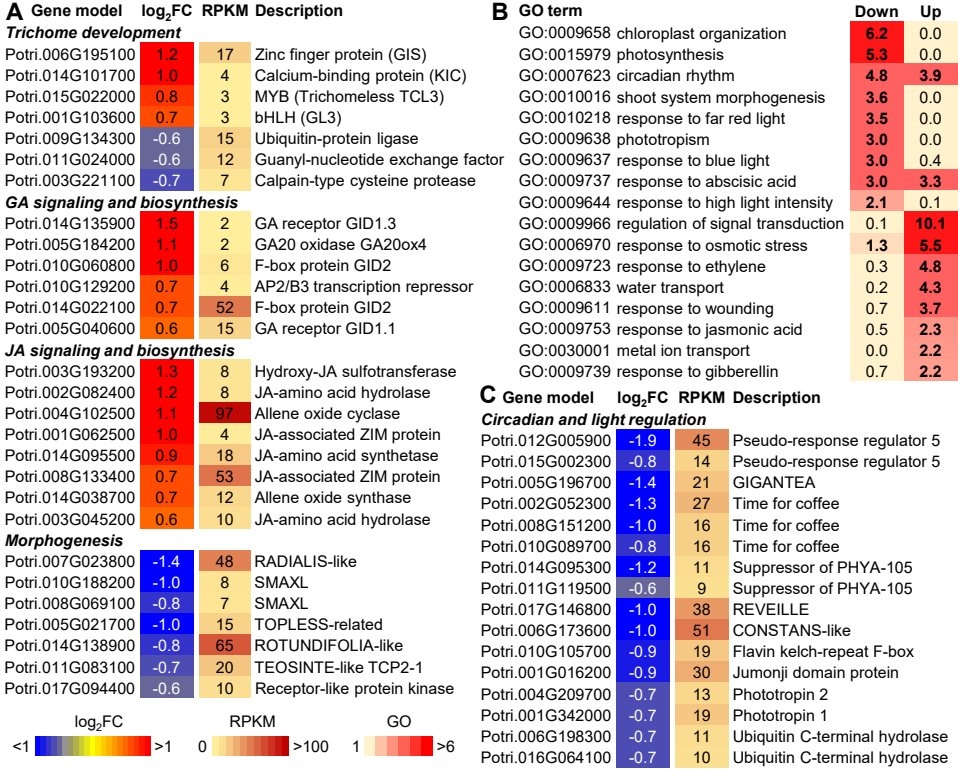

Figure 5. Transcriptional responses of trichomeless leaves. **A**, Expression response heatmaps of genes involved in trichome development, biosynthesis and signaling of GA and JA signaling and morphogenesis. **B**, Gene Ontology (GO) enrichment analysis of genes differentially up- or down-regulated in trichomeless leaves related to the control. Representative GO terms are visualized by the negative $\log_{10}$-transformed *P* values, with the color scales shown at the bottom. Boldfaced values indicate $P<0.05$). **C**, Expression heatmaps of genes involved in regulation of circadian rhythm and light responses. Expression responses in A and C are shown in $\log_2$-transformed fold-change (FC, mutant/control) and visualized according to the color scales at the bottom. Average basal expression levels from control samples are shown in RPKM (reads per kilobase of transcript per million mapped reads) and visualized according to the color scales at the bottom.

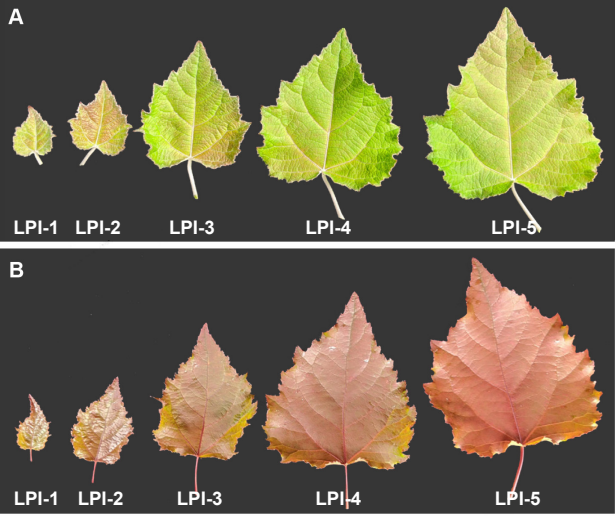

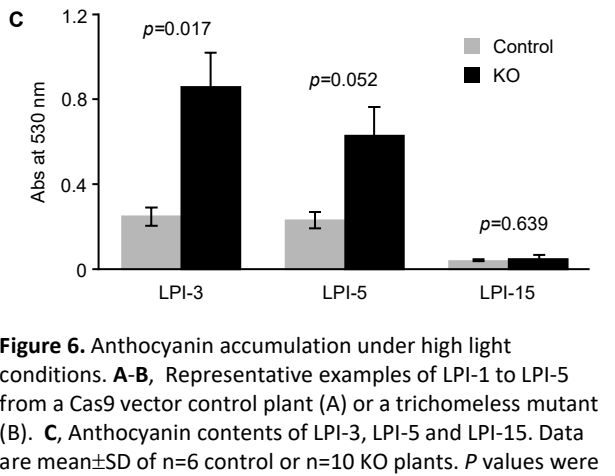

Figure 6. Anthocyanin accumulation under high light conditions. **A**-**B**, Representative examples of LPI-1 to LPI-5 from a Cas9 vector control plant (A) or a trichomeless mutant (B). **C**, Anthocyanin contents of LPI-3, LPI-5 and LPI-15. Data are mean±SD of n=6 control or n=10 KO plants. *P* values were determined using 2-tailed *t*-test.

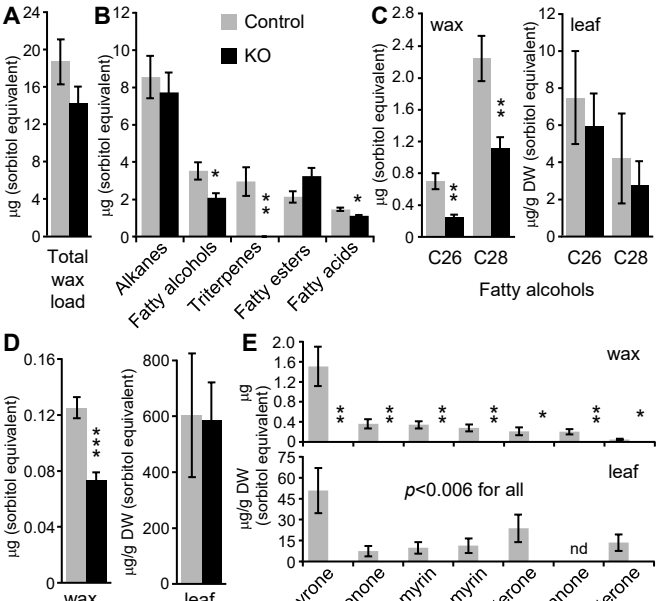

F

Gene model	log$_2$FC	RPKM	Description
Potri.006G101500	-1.0	91	Omega-3 fatty acid desaturase
Potri.016G117500	0.8	4	Omega-3 fatty acid desaturase
Potri.014G091800	-1.3	51	Delta-8 fatty acid desaturase
Potri.002G165800*	-0.6	9	Delta-8 fatty acid desaturase
Potri.004G097500	-0.6	19	Delta-7-sterol-C5-desaturase (STE1.1)
Potri.017G116600*	0.0	20	Delta-7-sterol-C5-desaturase (STE1.2)
Potri.005G177500	-0.8	8	Long chain acyl-CoA synthetase
Potri.002G084100*	-0.3	10	Long chain acyl-CoA synthetase
Potri.004G185000	-1.1	6	Fatty acyl-CoA reductase (FAR3.1)
Potri.009G145000*	-0.4	10	Fatty acyl-CoA reductase (FAR3.2)

log$_2$FC: <1 >1 RPKM: 0 >100

Figure 7. Cuticular wax composition of trichomeless and control leaves. **A**, Total wax load. **B**, Major classes of cuticle wax. **C**, Fatty alcohols (C26, 1-hexacosanol; C28, 1-octacosanol) detected in wax (left) or whole leaves (right). **D**, β-sitosterol detected in wax (left) or whole leaves (right). **E**, Triterpenes detected in wax (top) or whole leaves (bottom). Ergosterone, 14,24-dimethyl-ergosta-8,25-dien-3-one; cycloartanone, 24-methylene cycloartan-3-one; lanosterone, lanosta-8,24-dien-3-one. Data are mean±SD of n=5. All concentration estimates were based on sorbitol equivalent. Statistical significance was determined by 2-tailed *t*-test (* $P<0.05$, ** $P<0.01$, *** $P<0.001$). nd, not detected. **F**, Expression response heatmaps of genes involved in fatty acid and wax biosynthesis. Data presentation is the same as in Figure 5.

Parsed Citations

Alexa A, Rahnenfuhrer J (2010) topGO: Enrichment Analysis for Gene Ontology. R package version 2.0.
Google Scholar: Author Only Title Only Author and Title

Bewg WP, Ci D, Tsai CJ (2018) Genome editing in trees: From multiple repair pathways to long-term stability. Frontiers in Plant Science 9: 1732
Google Scholar: Author Only Title Only Author and Title

Bickford CP (2016) Ecophysiology of leaf trichomes. Functional Plant Biology 43: 807-814
Google Scholar: Author Only Title Only Author and Title

Briggs WR, Beck CF, Cashmore AR, Christie JM, Hughes J, Jarillo JA, Kagawa T, Kanegae H, Liscum E, Nagatani A, Okada K, Salomon M, Rüdiger W, Sakai T, Takano M, Wada M, Watson JC (2001) The phototropin family of photoreceptors. Plant Cell 13: 993-997
Google Scholar: Author Only Title Only Author and Title

Catchen JM, Amores A, Hohenlohe P, Cresko W, Postlethwait JH (2011) Stacks: Building and genotyping loci de novo from short-read sequences. Genes Genomes Genetics 1: 171-182
Google Scholar: Author Only Title Only Author and Title

Cheng Y, Wang L, Abbas M, Huang X, Wang Q, Wu A, Wei H, Peng S, Dai X, Li Q (2021) MicroRNA319-mediated gene regulatory network impacts leaf development and morphogenesis in poplar. Forestry Research 1: 4
Google Scholar: Author Only Title Only Author and Title

Dellaporta SL, Wood J, Hicks JB (1983) A plant DNA minipreparation: Version II. Plant Molecular Biology Reporter 1: 19-21
Google Scholar: Author Only Title Only Author and Title

Dobin A, Gingeras TR (2015) Mapping RNA-seq reads with STAR. Curr Protoc Bioinformatics 51: 11.14.11-11.14.19
Google Scholar: Author Only Title Only Author and Title

dos Santos Tozin LR, de Melo Silva SC, Rodrigues TM (2016) Non-glandular trichomes in Lamiaceae and Verbenaceae species: Morphological and histochemical features indicate more than physical protection. New Zealand Journal of Botany 54: 446-457
Google Scholar: Author Only Title Only Author and Title

Downes BP, Stupar RM, Gingerich DJ, Vierstra RD (2003) The HECT ubiquitin-protein ligase (UPL) family in Arabidopsis: UPL3 has a specific role in trichome development. Plant Journal 35: 729-742
Google Scholar: Author Only Title Only Author and Title

Falginella L, Andre CM, Legay S, Lin-Wang K, Dare AP, Deng C, Rebstock R, Plunkett BJ, Guo L, Cipriani G, Espley RV (2021) Differential regulation of triterpene biosynthesis induced by an early failure in cuticle formation in apple. Horticulture Research 8: 75
Google Scholar: Author Only Title Only Author and Title

Fambrini M, Pugliesi C (2019) The dynamic genetic-hormonal regulatory network controlling the trichome development in leaves. Plants 8: 253
Google Scholar: Author Only Title Only Author and Title

Filichkin SA, Breton G, Priest HD, Dharmawardhana P, Jaiswal P, Fox SE, Michael TP, Chory J, Kay SA, Mockler TC (2011) Global profiling of rice and poplar transcriptomes highlights key conserved circadian-controlled pathways and cis-regulatory modules. PLoS One 6: e16907
Google Scholar: Author Only Title Only Author and Title

Folkers U, Berger J, Hülskamp M (1997) Cell morphogenesis of trichomes in Arabidopsis: Differential control of primary and secondary branching by branch initiation regulators and cell growth. Development 124: 3779-3786
Google Scholar: Author Only Title Only Author and Title

Gachotte D, Meens R, Benveniste P (1995) An Arabidopsis mutant deficient in sterol biosynthesis: Heterologous complementation by ERG 3 encoding a Δ7-sterol-C-5-desaturase from yeast. Plant Journal 8: 407-416
Google Scholar: Author Only Title Only Author and Title

Galletti R, Johnson KL, Scofield S, San-Bento R, Watt AM, Murray JA, Ingram GC (2015) DEFECTIVE KERNEL 1 promotes and maintains plant epidermal differentiation. Development 142: 1978-1983
Google Scholar: Author Only Title Only Author and Title

Gan Y, Kumimoto R, Liu C, Ratcliffe O, Yu H, Broun P (2006) GLABROUS INFLORESCENCE STEMS modulates the regulation by gibberellins of epidermal differentiation and shoot maturation in Arabidopsis. Plant Cell 18: 1383-1395
Google Scholar: Author Only Title Only Author and Title

Gilding EK, Marks MD (2010) Analysis of purified glabra3-shapeshifter trichomes reveals a role for NOECK in regulating early trichome morphogenic events. Plant Journal 64: 304-317
Google Scholar: Author Only Title Only Author and Title

Glover BJ, Perez-Rodriguez M, Martin C (1998) Development of several epidermal cell types can be specified by the same MYB-related plant transcription factor. Development 125: 3497-3508

Google Scholar: Author Only Title Only Author and Title

Hall A, Bastow RM, Davis SJ, Hanano S, McWatters HG, Hibberd V, Doyle MR, Sung S, Halliday KJ, Amasino RM, Millar AJ (2003) The TIME FOR COFFEE gene maintains the amplitude and timing of Arabidopsis circadian clocks. Plant Cell 15: 2719-2729
Google Scholar: Author Only Title Only Author and Title

Hamaguchi A, Yamashino T, Koizumi N, Kiba T, Kojima M, Sakakibara H, Mizuno T (2008) A small subfamily of Arabidopsis RADIALIS-LIKE SANT/MYB genes: A link to HOOKLESS1-mediated signal transduction during early morphogenesis. Bioscience, Biotechnology, and Biochemistry 72: 2687-2696
Google Scholar: Author Only Title Only Author and Title

Hegebarth D, Buschhaus C, Wu M, Bird D, Jetter R (2016) The composition of surface wax on trichomes of Arabidopsis thaliana differs from wax on other epidermal cells. Plant Journal 88: 762-774
Google Scholar: Author Only Title Only Author and Title

Holwerda EK, Thorne PG, Olson DG, Amador-Noguez D, Engle NL, Tschaplinski TJ, van Dijken JP, Lynd LR (2014) The exometabolome of Clostridium thermocellum reveals overflow metabolism at high cellulose loading. Biotechnology for Biofuels 7: 155
Google Scholar: Author Only Title Only Author and Title

Hülskamp M (2004) Plant trichomes: A model for cell differentiation. Nature Reviews: Molecular Cell Biology 5: 471-480
Google Scholar: Author Only Title Only Author and Title

Imaizumi T, Tran HG, Swartz TE, Briggs WR, Kay SA (2003) FKF1 is essential for photoperiodic-specific light signalling in Arabidopsis. Nature 426: 302-306
Google Scholar: Author Only Title Only Author and Title

Jacobs TB, LaFayette PR, Schmitz RJ, Parrott WA (2015) Targeted genome modifications in soybean with CRISPR/Cas9. BMC Biotechnology 15: 16
Google Scholar: Author Only Title Only Author and Title

Jakoby MJ, Falkenhan D, Mader MT, Brininstool G, Wischnitzki E, Platz N, Hudson A, Hulskamp M, Larkin J, Schnittger A (2008) Transcriptional profiling of mature Arabidopsis trichomes reveals that NOECK encodes the MIXTA-like transcriptional regulator MYB106. Plant Physiology 148: 1583-1602
Google Scholar: Author Only Title Only Author and Title

Jones MA, Covington MF, DiTacchio L, Vollmers C, Panda S, Harmer SL (2010) Jumonji domain protein JMJD5 functions in both the plant and human circadian systems. Proc Natl Acad Sci U S A 107: 21623-21628
Google Scholar: Author Only Title Only Author and Title

Karabourniotis G, Liakopoulos G, Nikolopoulos D, Bresta P (2020) Protective and defensive roles of non-glandular trichomes against multiple stresses: Structure–function coordination. Journal of Forestry Research 31: 1-12
Google Scholar: Author Only Title Only Author and Title

Koncz C, Schell J (1986) The promoter of TL-DNA gene 5 controls the tissue-specific expression of chimaeric genes carried by a novel type of Agrobacterium binary vector. Molecular & General Genetics 204: 383-396
Google Scholar: Author Only Title Only Author and Title

Lange BM, Srividya N (2019) Enzymology of monoterpene functionalization in glandular trichomes. Journal of Experimental Botany 70: 1095-1108
Google Scholar: Author Only Title Only Author and Title

Lange BM, Turner GW (2013) Terpenoid biosynthesis in trichomes - Current status and future opportunities. Plant Biotechnology Journal 11: 2-22
Google Scholar: Author Only Title Only Author and Title

Larkin JC, Brown ML, Schiefelbein J (2003) How do cells know what they want to be when they grow up? Lessons from epidermal patterning in Arabidopsis. Annual Review of Plant Biology 54: 403-430
Google Scholar: Author Only Title Only Author and Title

Liakopoulos G, Nikolopoulos D, Klouvatou A, Vekkos KA, Manetas Y, Karabourniotis G (2006) The photoprotective role of epidermal anthocyanins and surface pubescence in young leaves of grapevine (Vitis vinifera). Annals of Botany 98: 257-265
Google Scholar: Author Only Title Only Author and Title

Liao Y, Smyth GK, Shi W (2014) featureCounts: an efficient general purpose program for assigning sequence reads to genomic features. Bioinformatics 30: 923-930
Google Scholar: Author Only Title Only Author and Title

Long JA, Ohno C, Smith ZR, Meyerowitz EM (2006) TOPLESS regulates apical embryonic fate in Arabidopsis. Science 312: 1520-1523
Google Scholar: Author Only Title Only Author and Title

Love M, Huber W, Anders S (2014) Moderated estimation of fold change and dispersion for RNA-seq data with DESeq2. Genome Biology 15: 550
Google Scholar: Author Only Title Only Author and Title

Machado A, Wu Y, Yang Y, Llewellyn DJ, Dennis ES (2009) The MYB transcription factor GhMYB25 regulates early fibre and trichome development. The Plant Journal 59: 52-62
Google Scholar: Author Only Title Only Author and Title

Maes L, Goossens A (2010) Hormone-mediated promotion of trichome initiation in plants is conserved but utilizes species- and trichome-specific regulatory mechanisms. Plant Signaling & Behavior 5: 205-207
Google Scholar: Author Only Title Only Author and Title

Maes L, Inzé D, Goossens A (2008) Functional specialization of the TRANSPARENT TESTA GLABRA1 network allows differential hormonal control of laminal and marginal trichome initiation in Arabidopsis rosette leaves. Plant Physiol 148: 1453-1464
Google Scholar: Author Only Title Only Author and Title

Matías-Hernández L, Aguilar-Jaramillo AE, Cigliano RA, Sanseverino W, Pelaz S (2016) Flowering and trichome development share hormonal and transcription factor regulation. Journal of Experimental Botany 67: 1209-1219
Google Scholar: Author Only Title Only Author and Title

Matsushika A, Makino S, Kojima M, Mizuno T (2000) Circadian waves of expression of the APRR1/TOC1 family of pseudo-response regulators in Arabidopsis thaliana: Insight into the plant circadian clock. Plant Cell Physiology 41: 1002-1012
Google Scholar: Author Only Title Only Author and Title

Mauriat M, Moritz T (2009) Analyses of GA20ox- and GID1-over-expressing aspen suggest that gibberellins play two distinct roles in wood formation. Plant Journal 58: 989-1003
Google Scholar: Author Only Title Only Author and Title

Meilan R, Ma C (2006) Poplar (Populus spp.). In K Wang, ed, Agrobacterium Protocols Volume 2. Methods in Molecular Biology, Vol 344. Humana Press, Totowa, NJ
Google Scholar: Author Only Title Only Author and Title

Narita NN, Moore S, Horiguchi G, Kubo M, Demura T, Fukuda H, Goodrich J, Tsukaya H (2004) Overexpression of a novel small peptide ROTUNDIFOLIA4 decreases cell proliferation and alters leaf shape in Arabidopsis thaliana. Plant Journal 38: 699-713
Google Scholar: Author Only Title Only Author and Title

Neff MM, Chory J (1998) Genetic interactions between Phytochrome A, Phytochrome B, and Cryptochrome 1 during Arabidopsis development. Plant Physiology 118: 27-36
Google Scholar: Author Only Title Only Author and Title

Ni M (2005) Integration of light signaling with photoperiodic flowering and circadian rhythm. Cell Research 15: 559-566
Google Scholar: Author Only Title Only Author and Title

Oppenheimer DG, Pollock MA, Vacik J, Szymanski DB, Ericson B, Feldmann K, Marks MD (1997) Essential role of a kinesin-like protein in Arabidopsis trichome morphogenesis. Proceedings of the National Academy of Sciences of the United States of America 94: 6261-6266
Google Scholar: Author Only Title Only Author and Title

Oshima Y, Shikata M, Koyama T, Ohtsubo N, Mitsuda N, Ohme-Takagi M (2013) MIXTA-like transcription factors and WAX INDUCER1/SHINE1 coordinately regulate cuticle development in Arabidopsis and Torenia fournieri. Plant Cell 25: 1609-1624
Google Scholar: Author Only Title Only Author and Title

Park DH, Somers DE, Kim YS, Choy YH, Lim HK, Soh MS, Kim HJ, Kay SA, Nam HG (1999) Control of circadian rhythms and photoperiodic flowering by the Arabidopsis GIGANTEA gene. Science 285: 1579-1582
Google Scholar: Author Only Title Only Author and Title

Payne WW (1978) A glossary of plant hair terminology. Brittonia 30: 239-255
Google Scholar: Author Only Title Only Author and Title

Plett JM, Wilkins O, Campbell MM, Ralph SG, Regan S (2010) Endogenous overexpression of Populus MYB186 increases trichome density, improves insect pest resistance, and impacts plant growth. Plant Journal 64: 419-432
Google Scholar: Author Only Title Only Author and Title

Qi T, Song S, Ren Q, Wu D, Huang H, Chen Y, Fan M, Peng W, Ren C, Xie D (2011) The Jasmonate-ZIM-domain proteins interact with the WD-Repeat/bHLH/MYB complexes to regulate jasmonate-mediated anthocyanin accumulation and trichome initiation in Arabidopsis thaliana. Plant Cell 23: 1795-1814
Google Scholar: Author Only Title Only Author and Title

Qiu JL, Jilk R, Marks MD, Szymanski DB (2002) The Arabidopsis SPIKE1 gene is required for normal cell shape control and tissue development. Plant Cell 14: 101-118
Google Scholar: Author Only Title Only Author and Title

Ramsay NA, Glover BJ (2005) MYB-bHLH-WD40 protein complex and the evolution of cellular diversity. Trends in Plant Science 10: 63-70
Google Scholar: Author Only Title Only Author and Title

Reddy VS, Day IS, Thomas T, Reddy AS (2004) KIC, a novel Ca2+ binding protein with one EF-hand motif, interacts with a microtubule motor protein and regulates trichome morphogenesis. Plant Cell 16: 185-200

Google Scholar: Author Only Title Only Author and Title

Rowland O, Zheng H, Hepworth SR, Lam P, Jetter R, Kunst L (2006) CER4 encodes an alcohol-forming fatty acyl-coenzyme A reductase involved in cuticular wax production in Arabidopsis. Plant Physiology 142: 866-877
Google Scholar: Author Only Title Only Author and Title

Schuepp PH (1993) Leaf boundary layers. New Phytologist 125: 477-507
Google Scholar: Author Only Title Only Author and Title

Schuurink R, Tissier A (2020) Glandular trichomes: Micro-organs with model status? New Phytologist 225: 2251-2266
Google Scholar: Author Only Title Only Author and Title

Smillie RM, Hetherington SE (1999) Photoabatement by anthocyanin shields photosynthetic systems from light stress. Photosynthetica 36: 451-463
Google Scholar: Author Only Title Only Author and Title

Soetaert SSA, Van Neste CMF, Vandewoestyne ML, Head SR, A. G, Van Nieuwerburgh FCW, Deforce DLD (2013) Differential transcriptome analysis of glandular and filamentous trichomes in Artemisia annua. BMC Plant Biology 13: 220
Google Scholar: Author Only Title Only Author and Title

Soundappan I, Bennett T, Morffy N, Liang Y, Stanga JP, Abbas A, Leyser O, Nelson DC (2015) SMAX1-LIKE/D53 family members enable distinct MAX2-dependent responses to strigolactones and karrikins in Arabidopsis. Plant Cell 27: 3143-3159
Google Scholar: Author Only Title Only Author and Title

Tao Q, Guo D, Wei B, Zhang F, Pang C, Jiang H, Zhang J, Wei T, Gu H, Qu LJ, Qin G (2013) The TIE1 transcriptional repressor links TCP transcription factors with TOPLESS/TOPLESS-RELATED corepressors and modulates leaf development in Arabidopsis. Plant Cell 25: 421-437
Google Scholar: Author Only Title Only Author and Title

Thimmappa R, Geisler K, Louveau T, O'Maille P, Osbourn A (2014) Triterpene biosynthesis in plants. Annual Review of Plant Biology 65: 225-257
Google Scholar: Author Only Title Only Author and Title

Tuskan GA, DiFazio S, Jansson S, Bohlmann J, Grigoriev I, Hellsten U, Putnam N, Ralph S, Rombauts S, Salamov A, Schein J, Sterck L, Aerts A, Bhalerao RR, Bhalerao RP, Blaudez D, Boerjan W, Brun A, Brunner A, Busov V, Campbell M, Carlson J, Chalot M, Chapman J, Chen GL, Cooper D, Coutinho PM, Couturier J, Covert S, Cronk Q, Cunningham R, Davis J, Degroeve S, Dejardin A, dePamphilis C, Detter J, Dirks B, Dubchak I, Duplessis S, Ehlting J, Ellis B, Gendler K, Goodstein D, Gribskov M, Grimwood J, Groover A, Gunter L, Hamberger B, Heinze B, Helariutta Y, Henrissat B, Holligan D, Holt R, Huang W, Islam-Faridi N, Jones S, Jones-Rhoades M, Jorgensen R, Joshi C, Kangasjarvi J, Karlsson J, Kelleher C, Kirkpatrick R, Kirst M, Kohler A, Kalluri U, Larimer F, Leebens-Mack J, Leple JC, Locascio P, Lou Y, Lucas S, Martin F, Montanini B, Napoli C, Nelson DR, Nelson C, Nieminen K, Nilsson O, Pereda V, Peter G, Philippe R, Pilate G, Poliakov A, Razumovskaya J, Richardson P, Rinaldi C, Ritland K, Rouze P, Ryaboy D, Schmutz J, Schrader J, Segerman B, Shin H, Siddiqui A, Sterky F, Terry A, Tsai CJ, Uberbacher E, Unneberg P, Vahala J, Wall K, Wessler S, Yang G, Yin T, Douglas C, Marra M, Sandberg G, Van de Peer Y, Rokhsar D (2006) The genome of black cottonwood, Populus trichocarpa (Torr. & Gray). Science 313: 1596-1604
Google Scholar: Author Only Title Only Author and Title

Walker AR, Davison PA, Bolognesi-Winfield AC, James CM, Srinivasan N, Blundell TL, Esch JJ, Marks MD, Gray JC (1999) The TRANSPARENT TESTA GLABRA1 locus, which regulates trichome differentiation and anthocyanin biosynthesis in arabidopsis, encodes a WD40 repeat protein. Plant Cell 11: 1337-1349
Google Scholar: Author Only Title Only Author and Title

Wang B, Luo Q, Li Y, Yin L, Zhou N, Li X, Gan J, Dong A (2020) Structural insights into target DNA recognition by R2R3-MYB transcription factors. Nucleic Acids Research 48: 460-471
Google Scholar: Author Only Title Only Author and Title

Wang H-Q, Tuominen LK, Tsai C-J (2011) SLIM: A sliding linear model for estimating the proportion of true null hypotheses in datasets with dependence structures. Bioinformatics 27: 225-231
Google Scholar: Author Only Title Only Author and Title

Wang S, Chen J-G (2014) Regulation of cell fate determination by single-repeat R3 MYB transcription factors in Arabidopsis. Frontiers in Plant Science 5
Google Scholar: Author Only Title Only Author and Title

Wang S, Chen JG (2014) Regulation of cell fate determination by single-repeat R3 MYB transcription factors in Arabidopsis. Frontiers in Plant Science 5: 133
Google Scholar: Author Only Title Only Author and Title

Wang W, Wang Y, Zhang Q, Qi Y, Guo D (2009) Global characterization of Artemisia annua glandular trichome transcriptome using 454 pyrosequencing. BMC Genomics 10: 465
Google Scholar: Author Only Title Only Author and Title

Wen J, Lease KA, Walker JC (2004) DVL, a novel class of small polypeptides: Overexpression alters Arabidopsis development. Plant Journal 37: 668-677

Google Scholar: Author Only Title Only Author and Title

Widemann E, Miesch L, Lugan R, Holder E, Heinrich C, Aubert Y, Miesch M, Pinot F, Heitz T (2013) The amidohydrolases IAR3 and ILL6 contribute to jasmonoyl-isoleucine hormone turnover and generate 12-hydroxyjasmonic acid upon wounding in Arabidopsis leaves. Journal of Biological Chemistry 288: 31701-31714

Google Scholar: Author Only Title Only Author and Title

Wilkins O, Nahal H, Foong J, Provart NJ, Campbell MM (2009) Expansion and diversification of the Populus R2R3-MYB family of transcription factors. Plant Physiology 149: 981-993

Google Scholar: Author Only Title Only Author and Title

Xue L-J, Alabady MS, Mohebbi M, Tsai C-J (2015) Exploiting genome variation to improve next-generation sequencing data analysis and genome editing efficiency in Populus tremula x alba 717-1B4. Tree Genetics & Genomes 11: 82

Google Scholar: Author Only Title Only Author and Title

Xue LJ, Tsai CJ (2015) AGEseq: Analysis of genome editing by sequencing. Molecular Plant 8: 1428-1430

Google Scholar: Author Only Title Only Author and Title

Zhang B, Hülskamp M (2019) Evolutionary analysis of MBW function by phenotypic rescue in Arabidopsis thaliana. Frontiers in Plant Science 10

Google Scholar: Author Only Title Only Author and Title

Zhang F, Gonzalez A, Zhao M, Payne CT, Lloyd A (2003) A network of redundant bHLH proteins functions in all TTG1-dependent pathways of Arabidopsis. Development 130: 4859-4869

Google Scholar: Author Only Title Only Author and Title

Zhao M, Morohashi K, Hatlestad G, Grotewold E, Lloyd A (2008) The TTG1-bHLH-MYB complex controls trichome cell fate and patterning through direct targeting of regulatory loci. Development 135: 1991-1999

Google Scholar: Author Only Title Only Author and Title

Zhou X, Jacobs TB, Xue L-J, Harding SA, Tsai C-J (2015) Exploiting SNPs for biallelic CRISPR mutations in the outcrossing woody perennial Populus reveals 4-coumarate:CoA ligase specificity and redundancy. New Phytologist 208: 298-301

Google Scholar: Author Only Title Only Author and Title

Zwaenepoel A, Van de Peer Y (2018) wgd-simple command line tools for the analysis of ancient whole-genome duplications. Bioinformatics 35: 2153-2155

Google Scholar: Author Only Title Only Author and Title